Thesis

On

A Computational Study on Entropy Generation Minimization of Pipe Bending

Submitted by

Trupti Ranjan Behera

710CH1020

Under the Supervision of

Dr. Basudeb Munshi

In partial fulfillment for the award of the degree of

Masters of Technology (Dual Degree)

In Chemical Engineering

Department of Chemical Engineering

National Institute of Technology Rourkela

May 2015

NATIONAL INSTITUTE OF TECHNOLOGY

ROURKELA

CERTIFICATE

This is to certify that the project entitled "**A Computational Study on Entropy Generation Minimization of Pipe Bending"** submitted by Trupti Ranjan Behera (710CH1020) in partial fulfillment of the requirements for the award of Master of Technology (Dual degree) in Chemical engineering, Department of Chemical Engineering at National Institute of Technology, Rourkela is an authentic work carried out by him under my supervision and guidance.

To the best of my knowledge the matter embodied in this thesis has not been submitted to any other university/Institute for the award of any Degree.

Dr. Basudeb Munshi

Date: Department of Chemical Engineering

Place: Rourkela NIT Rourkela

ACKNOWLEDGEMENT

On the submission of my thesis entitled “A Computational Study on Entropy Generation Minimization of Pipe Bending” I would like to express my deep and sincere gratitude to my supervisor Dr**.** Basudeb Munshi, Department of Chemical Engineering, for his guidance constant motivation, valuable suggestions, encouragement and support during the course work.

I would like to take the opportunity to thank Mr. Akhilesh Khapre for his unconditional assistance and support. I would like to thank again Dr. Basudeb Munshi for arranging computational facility for numerical simulations.

I would offer my loving thanks to my friends Aslam, Ramya, Devipriya and Pallav who provided me with strength and moral support. I would like to thank all others who have consistently encouraged and gave me moral support, without whose help it would be difficult to finish this project.

Last but not the least, I would like to express my love, respect and thanks to my parents Mrs Kanchan Late Giri and Mr. Kshiroda Kumar Behera for being backbone of my life and for their unconditional love. Special thanks to my sister and brother.

Trupti Ranjan Behera

710CH1020

ABSTRACT

This project presents solution of a simple optimization problem of flow through circular bent channels. Six different bending angles of the pipe were taken for finding the effect of bending angle on the pressure drop. The diameter and length of all the pipes were taken same irrespective of the bending angles. The CFD model equations were solved to predict the hydrodynamic behaviour of pipe. The models were solved by ANSYS Fluent 15.0 solver. The CFD models were validated by comparing the computed pressure drop with the analytically computed pressure as given in the previous literature. The entropy generation rate was compared and the optimum bending angle was found by taking pressure drop across the pipe as reference. The entropy generations in both isothermal and non-isothermal conditions were studied and compared mutually for a particular flow rate. An EGM analysis was carried out and a thermodynamically optimal solution was identified. It was also observed that as the bending angle increases the entropy generation decreases for a particular flow rate.

Keywords: CFD, Entropy generation minimization, Pipe bending

Contents

LIST OF FIGURES

LIST OF TABLES

NOMENCLATURE

S= Entropy

CFD= Computational Fluid Dynamics

Re= Reynolds Number

A= Bending Angle

EGM= Entropy Generation Minimization

S'''_{gen}= Volumetric Entropy Generation

CHAPTER-1

INTRODUCTION

1.1 Energy

Energy is everywhere. Anything we eat or use has energy in it. Everything that we process or every object we produce requires energy, and the economic growth of a country is related to the energy demands. But during an engineering operation most of the energy is not utilized so it transforms to another form and loss of energy occurs. As the world energy situation is getting more and more serious, the optimization of thermal systems attracts increasing attention because about 80% of the total energy consumption is related to heat and improving the performance of thermal systems is of great significance to the energy conservation [1].

1.2 Entropy

Entropy is the degree to which energy is wasted. While the exergy of a system is the maximum work possible during a process. So the amount of available work (or exergy) depends on the amount of entropy produced [2]. The amount of entropy generated can be directly used as an efficiency parameter of the system. Minimization of entropy generation in a thermodynamic system provides efficient use of exergy that is available.

1.3 Entropy Generation Minimization (EGM)

The theorem of minimum entropy generation says that, under certain assumptions, the global entropy production rate of a given system attains a minimum value when the processes in the system become stationary. This method combines the most fundamental principles of thermodynamics, heat transfer, and fluid mechanics [2].

Bejan [2] studied minimization of entropy generation in heat exchangers, insulation systems, storage system, power generation, refrigeration processes in brief. But later on many more detailed analysis of his work is carried out by many authors.

1.4 Mass transfer Studies using EGM

Like in mass transfer operations, Barbosa et al. [16] have optimized the finned tube evaporator using the Entropy generation minimization (EGM) principle. While Özyurt et al. optimized evaporator for use in a refrigeration cycle [17]. For condensation of gases in the presence of high non-condensable gases, in the design of fan-supplied tube-fin condensers and Refrigerant circuitry design of tube condenser different authors used EGM as efficiency parameter [18-20]. Ng et al., [21] analyzed the EGM of absorption chiller. Mistry et al. [22] used entropy generation as a parameter to analyze the desalination process.

1.5 Nano-Fluid Flow and heat transfer Using EGM

In nanofluid flow, Leong et al. [41] and [42] analyzed entropy generation of three different types of heat exchangers studying the turbulent convection of nanofluids subjected to constant wall temperature. Singh et al. [44] And Bianco et al. [43] theoretically investigated entropy generation of nanofluids convection and showed the existence of different optimal working points according to the flow features without considering the influence of particles diameter. Bianco et al. [45] numerically developed turbulent forced convection flow in a square tube, subjected to constant and uniform wall heat flux of a water–Al_2O_3 nanofluid. Bianco and Manca [46] proposed a simple analytical procedure to evaluate the entropy generation and showed that it takes a good agreement with the numerical calculations.

1.6 Heat transfer and flow through a channel using EGM

Sahin [5] considered a range of laminar streams at steady heat flux boundary condition and explored different pipe geometries to minimize the entropy losses. Among different geometries, when the frictional contribution of entropy generation are prevailing round geometry is the best. Dagtekin et al.[6], Oztop [7] studied the effect of longitudinal blades of diverse shapes for laminar stream in a circular conduit and demonstrated that the cross-sectional region and the wall heat flux have extensive impact on entropy generation. For improved heat exchange surfaces of a tubular heat exchanger at steady wall temperature Zimparov [8] concentrated on liquid temperature variety along the length of exchanger by creating execution assessment criteria mathematical equations taking into account the entropy generation hypothesis. Mahmud and Fraser [9] concentrated on channel with circular cross-sectional area and between two parallel plates and investigated second law attributes of heat exchange and liquid stream because of

constrained convection. Sahin [10] demonstrated that consistency variety had an extensive impact on both entropy generation and pumping power. Thermodynamic enhancement of convective heat move in a funnel with consistent wall temperature has been considered by Mukherjee [11], Esfahani and Alizadeh [13] and Sahin [12]. Esfahani They discovered a relationship between ideal estimations of Stanton number and the proportion of the length of the funnel to its width (St.L/D). Sahin et al. [14] numerical dissected the impact of fouling on operational cost in channel stream on entropy generation. Sahin [15] additionally upgraded the measure of heat exchanger and the channel temperature of the liquid for which the aggregate irreversibility because of heat exchange and weight drop turns into the base by examining entropy generation for a laminar thick stream in a conduit subjected to consistent divider temperature. Esfahani et al. [4] broke down the impact of non-uniform heating in laminar stream on entropy generation.

1.7 Motivation

. There is an increased need for utilization of a variety of duct geometries for internal flow heat transfer applications along with the advancement of science and technology. Due to the size and volume constraints in the areas of electronics, biomedical, atomic, and aviation, it may be required to use different flow passage geometries.

Up to now several studies have been done taking geometrical factors into account to calculate the Entropy generation rate. For example Sahin [5] took different geometries like rectangular, circular, triangular, sinusoidal and square to analyze the flow through the channel. Hilbert and Mercus [36] [37], calculated the pressure drop in tee bending, short radius elbow and long radius elbow of channel flow but considered only bending angle to be 90^0. Sciubba [35] studied the viscous dissipation effect of bifurcation of a channel on entropy generation.

But no one has studied the effect of bending angle on pressure drop and entropy generation. So this study is to analyze the effects of various bending angles on different parameters.

1.8 Objective of the work

- Validation for pressure drop across the pipe inlet and outlet for various Re number.
- To find out the effect of Re on pressure drop across the pipe ends
- To find out the effect of Re on entropy generation for iso-thermal (constant temperature and same of liquids and wall) problems.

- To find out the effect of Re on entropy generation for constant heat flux boundary condition case.
- To find out the effect of Re on entropy generation for non-isothermal constant wall temperature case.

CHAPTER-2

LITERATURE REVIEW

2.1 Pressure drop in Channels

Hilbert[36] examined three bends: blinded tee, short radius elbow and long radius elbow experimentally. He found that from the standing point of the wear the blinded tee is the best bend followed by short radius elbow and long radius sweep is the least preferable one.

Marcus et al.[37] measured the pressure loss of the three bends and found that for a wide range of mass flow ratio short radius elbows provides the lowest pressure loss for fine powdered materials.

2.2 Entropy Generation analysis in Mass Trasfer Applications

Lienhard et al. [22] analyzed desalination process considering the separation work along with it lost work due to entropy generation. Entropy generated due to irreversibility in the separation process, along with the irreversible mixing of the brine with the ambient seawater and temperature disequilibrium of the discharge. The entropy generation due to chemical disequilibrium was found to be important for systems with high recovery ratios.

2.3 Entropy Generation analysis of Nano-Fluid Flow

Manca et al. [45] investigated the entropy generation in turbulent forced convection flow of Al_2O_3–water nano fluid at constant wall heat flux boundary condition. For a constant Reynolds number, nanoparticles were added to decrease entropy generation. The optimal concentration reduced with increase of Re. The reduction of velocity decreased entropy generation due to friction. Total entropy generation was reduced by very small concentration of the nano-fluids due to the increase of nano-fluid thermal conductivity. When constant inlet velocity condition was considered, by increasing the concentration of the nano-fluid, entropy generation rate was increased, because viscosity effect began to predominate, Re was reduced and consequently total entropy generation rate was increased.

Singh et al. [44] analysed entropy generation of nanofluids of two different viscosity models, while considering conductivity, for laminar and turbulent flow. They have found that an

optimum diameter at which the entropy generation rate was occurred was less for laminar flow in comparison to turbulent flow. The entropy generation ratio was found to be always greater than one and it increased with volume fraction for laminar flow. But the behaviour was found to be opposite for turbulent flow. The viscous entropy generation part decreased with volume fraction, while thermal part increased with volume fraction. At smaller diameter, the viscous entropy generation part has higher values and at higher diameters, the thermal part of entropy generation has. The entropy generation rate increased very slowly or became constant after a particular diameter.

Leong et al. [41] analyzed the entropy generation of nanofluid. As the volume fraction of the nanaoparticle was increased total dimensionless entropy generation was decreased. When Titanium dioxide nanofluids and alumina nano-fluids were compared for lower dimensionless entropy generation value, titanium dioxide nanofluids showed good results. As the dimensionless temperature difference was increased, total dimensionless entropy generation also increased. Mass flow rate of Titanium dioxide or alumina nanofluid influenced the total dimensionless entropy generation.

Leong et al. [42] also studied different types of heat exchangers using nanofluids as working fluid. Shell and tube heat exchanger with case of helical baffles (25°) showed highest overall heat transfer coefficient. But when the mass flow rate was increased the result also came the same followed by segmental and helical baffles (50°). When the nanoparticles were added the overall heat transfer coefficient was increased but it was found to be independent of the types of heat exchanger. The HTC for heat exchanger with 25° helical baffles was the highest so the heat transfer rate compared to that of segmental and 50° helical exchanger. Entropy generation was minimized for the 50° helical exchanger due to its lowest total pressure drop.

2.4 Flow through Microchannels

Ibáñeze et al. [30] optimized various flows in a parallel plate microchannel having finite wall thickness using the entropy generation minimization method. An optimum slip velocity was obtained which was leading to a minimum entropy generation rate and they analyzed effects of slip velocity on the optimum values of some other parameters. Besides all these the Nusselt number was also calculated and analyzed. An optimum value of the slip length for which the heat transfer was maximized was derived.

Ibáñez et al. [31] illustrated the combined effects of slip flow and wall heat on entropy generation in a microchannel. The entropy generation reached a minimum for the wall heat flux for geometrical and physical parameters of the system and wall-fluid thermal conductivity ratio. The optimum values of both the slip flow and wall to fluid thermal conductivity ratio, where the entropy generation was minimum, decreased with the wall heat flux. Finally, these minimum values of entropy, reached in the optimum values of slip flow and wall to fluid thermal conductivity ratio.

Hung et al. [32] developed analytical model of water-alumina nanofluid flow in circular microchannels and investigated the effects of nanoparticle suspension, microchannel aspect ratio, and stream-wise conduction in low-Peclet-number flow regime on the entropy generation. Stream-wise conduction affected the thermal characteristics of the nanofluids, and consequently the entropy generation but its effect due to fluid friction irreversibility was not significant. When nanoparticle suspension increased the heat transfer irreversibility was dominant. In certain range of low Peclet number flow at optimum condition for nanofluid flow in microchannels minimal entropy generation was identified. The aspect ratio of the microchannel affected the second-law performance of nanofluid prominently. By increase in the aspect ratio was found to effectively enhance the exergetic effectiveness of the flow when the heat transfer irreversibility was dominant. When the fluid friction irreversibility was dominant, the choice of working fluid was more important than the design of the microchannel.

Anand [33] analyzed the thermally fully developed flow with viscous dissipation of a non-Newtonian fluid through a microchannel. The effect of slip on heat transfer and entropy generation was important and could not be neglected, especially for shear thickening fluids ($n > 1$) the curves for velocity distribution and temperature distribution had higher slopes, especially towards the centerline of the channel, in comparison to shear thinning fluids. The slip parameters only affected the advection of fluid momentum and not its diffusion For symmetrical slip boundary conditions. Average entropy generation rate was lower than the corresponding values predicted by asymptotic slip law for shear thickening fluids; and this difference increased with increase in the value of slip coefficients. The Bejan number for shear thickening fluids was much less than that for shear thinning fluids and $Be < 0.5$ throughout the channel width so we can say that for shear thickening fluids, most of the irreversibility was due to fluid friction. Thus to minimize the entropy generation for power law fluids, for shear thickening fluids

concentration should be on friction irreversibility and for shear thickening fluids on heat transfer irreversibility. For shear thinning fluids (n<1), Bejan number tends to 1 at axis of symmetry, while for shear thickening fluids (n>1), Bejan number tends to 0.

Huai et al. [34] numerically investigated the effect of viscous dissipation on total entropy generation for curved square microchannles in the laminar flow region by using two different working fluids. The working fluids were aniline and ethylene glycol. The effect of viscous dissipation was studied and analyzed to calculate the total entropy generation number and heat transfer entropy generation number. When the case of cooled fluid was considered heat transfer entropy generation number and the frictional entropy generation number were decreased due to the viscous dissipation effect. The Bejan number was found to be lower when the working fluid aniline was heated than to cooling. The curved microchannels having smaller curvature radius showed earlier total entropy generation number minimization, and the Bejan number generally reduced as the curvature radius diminished. The heat transfer entropy generation number decreased with Reynolds number. The total entropy generation number extremum did not appear, for the case of ethylene glycol at large Reynolds number region when it was heated under viscous dissipation effect. Throughout the study they have found that the frictional entropy generation dominated the total entropy generation.

2.5 EGM analysis for pipe or channel flow

A number of studies have been done on entropy generation in fluid flow and heat transfer problems. Bejan showed that the entropy generation is due to heat transfer and viscous friction for forced convection viscous fluid flow in a channel. He also showed that when the entropy generation is minimized, for the case of heat transfer in a circular tube, a relation exists between heat transfer and viscosity effects of the components of entropy generation associated with it. Bejan also applied the concept of minimum entropy generation to the design of a counter-flow heat exchanger. He showed that an optimum flow path length would be possible [3] [4] [2].

Bertola and Cafaro [23] reviewed the principle of minimum entropy production of fluid at rest by the heat conduction and the combined effect of heat conduction and shear flow in an incompressible fluid flow. This theorem was a best approximation method and as the system converged to equilibrium it converged to the exact solution. And for a system in a stationary state the entropy production was approximately zero.

Sahin [5] compared entropy generation and pumping power required for different duct geometry for optimum shape with constant wall temperature boundary condition. Duct geometries used are: square, circular, rectangle, equilateral triangle, and sinusoidal. The optimum duct geometry depends on the Reynolds number. Circular duct geometry proves to be the optimum when the entropy generation was mostly contributed by frictional losses. Rectangular duct would gave the best result when the ratio between length to width or the aspect ratio became one. From the point of view of entropy generation for low Re number region sinusoidal duct geometry appeared to be the best, but the pumping power requirement for the sinusoidal geometry was higher than that for the square geometry.

Vučković et al. [24], studies on the numerical simulation of local entropy generation rate in flow meter and pipeline curve. The results of numerical simulation show good agreement with measured data in regard to temperature. The friction factor of irreversibility is more influence on the generation of entropy than heat transfer irreversibility.

Mahmud and Fraser [9] studied the forced convection inside channel with circular cross-section and channel of parallel plates having finite gap in between them at iso-flux and isothermal boundary conditions. Along with the Newtonian fluid they considered Non-Newtonian fluid flow in the above boundary condition. Entropy generation number and Bejan number were derived analytically for each case of axial conduction, heat transfer normal to the axis and fluid frictional irreversibility. And then he studied the Bejan no/entropy gen in axial, radial and different directions.

Sahin [10] studied numerically the entropy generation rate in a developing laminar viscous fluid flow in a circular pipe with variable viscosity and constant heat flux boundary condition. The entropy generation rate is higher near the wall and decreases along the radius away from the surface of the pipe as the temperature and viscosity gradient are high near the wall of the pipe. Around the centerline of the pipe viscosity and temperature gradients are small and hence the entropy generation was small. The viscosity variation affects velocity and the temperature profiles, as well as the entropy generation rate. Axial variation of the entropy generation rate near the wall sharply increased to a maximum and then steadily decreased. The integrated value of entropy generation rate increased over the cross-sectional area of the pipe due to the

temperature penetration and the widening of the thermal as well as hydrodynamic boundary layers.

Abolfazli and Alizadeh [13] have also studied the thermodynamic optimization of geometry in convective heat transfer at constant temperature at the wall by considering laminar flow. They found out the effects of different parameter on the pumping power and Entropy generation. They also introduced a proper correlation for the optimum design of the tube.

Sahin [12] wrote the dimensionless entropy generation and pumping power to heat transfer ratio as functions of three dimensionless numbers, using an average heat transfer coefficient and a friction factor at average bulk temperature. The entropy generation per unit heat transfer rate decreased with duct length, while the entropy generation per unit capacity rate increased. On the other hand when the variation of viscosity with temperature was considered, the pumping power to heat transfer ratio decreased with duct length. As the dimensionless wall heat flux is increased, entropy generation per unit heat transfer rate and entropy generation per unit heat capacity decrease initially reaching a minimum for the case of variable viscosity model and then increase. As the wall heat flux decreases, pumping power to heat transfer ratio may increase very sharply for viscous fluids.

Sahin [15] studied entropy generation rate in a developing laminar viscous fluid flow in a circular pipe with iso-flux boundary condition. Near the wall the entropy generation rate was higher and sharply decreases along the radius away from the surface of the pipe. This happens so because of the existence of the velocity and temperature gradients in the region of the pipe. Around the centerline entropy generation rate was small because of the small temperature and velocity gradients. Thermal component contribution to the entropy generation rate was high. Along the axial direction near the wall the entropy generation rate was very high and reaches maximum then decreases steadily. Due to flux, temperature penetration occurred into the working fluid. Along with it hydrodynamic boundary layer and thermal boundary layer got widened. So the entropy generation rate along the axial direction over the cross sectional area of the pipe increased steadily.

Sahin [14] also studied the effect of fouling due to heat transfer and pressure drop in viscous pipe flow on the irreversibility components. He found that the increase in the irreversibility due to heat transfer was slower than that due to viscous friction. As the fouling layer build up, total cost

due to irreversibility reached a minimum and after that it increased. The fouling layer thickness depends upon the cost ratio. The optimum thickness dropped as the cost ratio was increased. The cost of irreversibility was found to be dependent and directly proportional to the temperature difference between the tube wall and inlet fluid. He suggested that by considering the cost variation versus fouling layer thickness excessive cost due to the irreversibility can be avoided.

Jankowski [27] analyzed and generalized entropy generation in fully-developed convective heat transfer flow. He made the correlations to determine the optimum cross-sectional shape of a flow passage. The circular cross-section minimized flow resistance hence the entropy generation minimization occurs. From the heat transfer correlations he suggested that the circular cross-section was not always ideal. For a duct with a large wetted perimeter has more surface area available for heat transfer so the heat transfer irreversibility component dominated and minimization of the overall entropy generation occurred.

Sahin and Yilbas [28] studied the flow between the parallel plates and of the bi-vertical motion of the top plate and its effect on entropy generation. By increasing the velocity of the plate, the entropy generation rate lowers. When they kept the velocity constant the entropy was found to take shape of an exponent and when the force was kept constant the entropy took the shape of a parabola. In the flow system combination of those two steps results in the minimum entropy generation. At specific displacement value minimum entropy occurred. Constant velocity operation should was allowed to reach a particular gab height of the plates before the constant applied force. Consequently, combination of the two cases provided the minimum power loss and minimum entropy generation in the working fluid between the two plates considered.

Sciubba.[35] studied the entropy generation rate due to viscous dissipation for three cases: (a) a single bifurcation, (b) a straight tube with wall suction, and (c) bifurcation with wall suction. For laminar bifurcation without losses the entropy generation rate depended strongly upon the aspect ratio. For any bifurcation length, constant velocity case showed a lower entropy generation rate than the constant Re case. For each physical situation of constant Re and constant inlet velocity a optimal configuration was existed and it displayed minimum value of the entropy generation rate. For the examined situations, a configuration existed that showed the lowest viscous entropy generation rate which was found to be compatible with the imposed constraints.

Jarungthammachote [29] studied, the entropy generation of transient heat conduction with fixed temperature boundary conditions. For heating case the maximum non-dimensional entropy generation rate takes place near the surface and its value reduces with increase of time because of high temperature gradient near the surface. Initial temperature has very weak effect on total entropy generation rate. When time increases the effect of initial condition disappears and as the time approaches infinity, the temperature distribution, the local entropy generation rate, and the total entropy generation rate of transient problem are approach those of steady state problem.

2.6 Entropy Generation analysis for Heat exchangers

Dagtekin et al.,[6] Measured the entropy generation and the pumping power variations for laminar flow and constant wall temperature conditions in a circular duct with longitudinal thin, triangular and V-shaped fins respectively. The inlet to wall temperature difference was found to be a function of entropy generation, and increased with increase if the temperature difference. As the number of the fins or length of the fins was increased, the dimensionless entropy generation was also increased. When the higher values of the Reynolds number were considered, the entropy generation for thin fins was found to be superior to triangular fins. While triangular fins were considered by gradually increasing the fin angle, entropy generation to heat transfer ratio increased. While for V-shaped fins, with the increase of the fin angle the entropy generation and the pumping power to heat transfer ratio both were increased.

Tandiroglu [25] investigated a transient turbulent flow in a circular pipe with baffle inserted into it and studied the characteristics of forced convection and entropy generation with constant heat flux condition and proposed a correlation. He suggested that the baffle inserted tubes of type 4562 to be preferred for the best performance because it exhibited the minimum time averaged entropy generation number for transient forced convection flow conditions based on experimental data and correlations for time averaged entropy generation number.

Oztop [7] analyzed the second law of thermodynamics of laminar flow subjected to constant wall heat flux for semi-circular ducts. As Reynolds number or temperature difference is increased total entropy generation is decreased. Contingent upon Reynolds number and when cross-sectional area is expanded aggregate entropy generation is expanding for the same Reynolds number. Further, an increment in cross-sectional area reasons to build obliged pumping power.

Zimparov [8] studied heat transfer and fluid friction characteristics of 10 spirally corrugated tubes to illustrate the application of the extended performance evaluation criteria equations. The results for different design constraints show that the optimum rib-height-to-diameter ratio (e/D) for spirally corrugated tubes is about 0.04 and the entropy generation value is minimum for this case. An augmentation technique is utilized in a heat exchanger to improve its performance characteristics, more significant benefits can be obtained if it operates at constant wall temperature.

Nag and Mukherjee [11] studied heat transfer from a duct with constant wall temperature during phase change on one side of a heat exchanger tube. The important design criteria was the initial temperature difference The heat transfer to pumping power ratio was used at its optimum value. Simply maximizing this ratio of pumping power to heat transfer is not often a good solution, because sometimes a large amount of energy may be irreversibly lost and the entropy generated may be far from the minimum possible.

The common closed thermodynamic systems like Carnot cycle and refrigeration cycles etc. are analyzed with the concepts of dimensionless entropy generations by Cheng and Linag [26]. They found that when the entropy generation number was small the larger is the exergy-work conversion efficiency. It is found that a percentage of the given mechanical work turns to be the net exergy stream into the heat sources, while the rest is destructed in view of entropy generation. At the point when the net exergy stream rate into the heat sources is altered, littler entropy generation rate leads littler information force, while it prompts bigger net exergy stream rate into the heat energy for settled input power.

CHAPTER-3

GOVERNING EQUATIONS

3.1 COMPUTATIONAL FLUID DYNAMICS:

Having the capacity to concoct proficient and ideal outlines for new items is one of the greatest difficulties in the building processes. One of the most grounded devices in this classification is FLUENT. Familiar is an exceptionally helpful system procured by ANSYS. It has the ability to model liquid move through articles, past items and numerous more and the capacity to test, break down results and outline under one system.

ANSYS Familiar is Computational Liquid Motion (CFD) programming. It permits users to simulate flow issues of running multifaceted nature. It has wide physical modeling abilities by which planning of the model flow, turbulence, heat transfer, and reactions over objects is done by the user. From the utilization of CFD programming as a fundamental piece of their outline stages a great many organizations has been profited in their item advancement. It utilizes the finite volume method to comprehend the representing Navier-Stokes mathematical statements for a liquid. Navier-stokes equations are gotten from (1) the mass conservation equation, (2) the preservation of energy equation and (3) the preservation of momentum equation.

$$\frac{\partial \rho}{\partial t} + \nabla \cdot \left(\rho \vec{V}\right) = 0 \qquad 1$$

$$\rho \frac{\partial \vec{V}}{\partial t} + \rho\left(\vec{V} \cdot \nabla\right)\vec{V} = -\nabla\rho + \rho\vec{g} + \nabla \cdot \tau_{ij} \qquad 2$$

$$\frac{\partial}{\partial t}\int e * \rho \, d\forall + \int (\breve{u} + \frac{p}{\rho} + \frac{V^2}{2} + gz)\rho \boldsymbol{V} \cdot \breve{\boldsymbol{n}} \, \mathrm{dA} = \dot{Q_{net\ in}} + \dot{W_{net\ in}} \qquad 3$$

The preservation of mass, momentum and energy are coupled and non-linear arrangement of differential mathematical statements. It is for all intents and purposes difficult to tackle the above comparisons systematically for useful engineering issues. So the difficulty arises. But CFD software FLUENT provides approximation to solve the specified governing equations.

FLUENT also allows to model flows such as compressible or incompressible, viscous or invisid, turbulent or laminar flow. It has flexible moving and deforming meshes through which fast and

accurate results are obtained to create optimal designs. Ultimately, FLUENT allows engineers to design, create and analyze a configuration all under one program.

To model the object that a user wants to work with, its geometry and mesh must be first created in ANSYS Workbench and the meshing implementation can be done in the specimen to analyze the structure as they try to analyze fluid flow through or past the object.

A couple of diverse methods for displaying and investigating liquid flow are through turbulence modeling, k-ε, and Y+. To model turbulent flow turbulence modeling is used. Large, nearly random fluctuations in velocity and pressure in both space and time are the characters of turbulent flow. The fluctuations arised from the turbulent instability are dissipated into heat by viscosity or viscous dissipation. In the opposite limit of high Reynolds numbers turbulent flows occur. There are two approaches to solving the turbulent flow equations, direct numerical simulations and k-ε. In immediate numerical simulation the Navier-Stokes equations is specifically integrated, determining the majority of the spatial and transient changes without turning to displaying yet in k-ε, models Reynolds push in two turbulent parameters, the turbulent kinetic energy (k) and the turbulent dissipation rate characterized beneath by Mathematical statements 4 and 5 respectively.

$$\kappa \equiv \frac{1}{2}\left(\overline{u'^2} + \overline{v'^2} + \overline{w'^2}\right) \qquad 4$$

$$\epsilon \equiv \upsilon[\left(\frac{\partial u'}{\partial x}\right)^2 + \left(\frac{\partial u'}{\partial y}\right)^2 + \left(\frac{\partial u'}{\partial z}\right)^2 + \left(\frac{\partial v'}{\partial x}\right)^2 + \left(\frac{\partial v'}{\partial y}\right)^2 + \left(\frac{\partial v'}{\partial z}\right)^2 + \left(\frac{\partial w'}{\partial x}\right)^2 + \left(\frac{\partial w'}{\partial y}\right)^2 + \left(\frac{\partial w'}{\partial z}\right)^2 \qquad 5$$

As the complexity in the geometries of the design increase it is required to adjust the meshing accordingly. The CFD software codes solve directly the flow variables at each element and the values at other locations are interpolated. Where there more flow gradients occurring around a certain area rather than a complicated geometry one can concentrate the mesh around a certain area.

Enhanced wall treatment is another modeling capability FLUENT uses. It is especially used for turbulent cases using the k-epsilon model as it analyzes the object closer near the wall region. The initial and boundary conditions are specified in FLUENT. And after initializing the problem;

convergence is checked. If the convergence is not achieved accurate results will not be obtained. Finally, FLUENT provides a wide variety of parameters that can be plotted and analyzed.

Let us consider the finite-difference method in 1D. If the grid has equally-spaced points with Δx being the spacing between successive points, the truncation error is O (Δx). As the number of grid points is increased, and the spacing between successive points is reduced, the error in the numerical solution would decrease. Therefore the obtained numerical solution will closely agree to the exact solution. In FLUENT for the convergence the governing equations are solved for a number of iterations. The magnitude of the average of variable is computed by Navier Stokes equation and Equation 6.

$$R = \sqrt{\frac{\sum_{i=1}^{N}(u_i - u_{gi})^2}{N}} \qquad 6$$

where u indicates a particulate variable to be computed, N is the number of iterations to be performed, R is the residual, and the subscript g indicates a guessed value.

3.2 Laminar and turbulent flow into the pipe:

FLUENT is a very powerful tool in obtaining solutions to a wide range of fluid flow problems. The results obtained should be carefully validated with known theory or empirical data to make sure they are accurate. For example, for the flow through a pipe, the pressure drop obtained can be compared with the empirical formulae. For a steady state laminar flow and turbulent flow in circular tubes the Navier-Stokes upon making the necessary assumptions can be solved. The incompressible Navier-Stokes equations in Cartesian coordinates are shown in Equations 7, 8 and 9.

$$\rho\left(\frac{\partial u}{\partial t} + u\frac{\partial u}{\partial x} + v\frac{\partial u}{\partial y} + w\frac{\partial u}{\partial z}\right) = -\frac{\partial p}{\partial x} + \rho g_x + \mu\left(\frac{\partial^2 u}{\partial x^2} + \frac{\partial^2 u}{\partial y^2} + \frac{\partial^2 u}{\partial z^2}\right) \qquad 7$$

$$\rho\left(\frac{\partial v}{\partial t} + u\frac{\partial v}{\partial x} + v\frac{\partial v}{\partial y} + w\frac{\partial v}{\partial z}\right) = -\frac{\partial p}{\partial y} + \rho g_y + \mu\left(\frac{\partial^2 v}{\partial x^2} + \frac{\partial^2 v}{\partial y^2} + \frac{\partial^2 v}{\partial z^2}\right) \qquad 8$$

$$\rho\left(\frac{\partial u}{\partial t} + u\frac{\partial w}{\partial x} + v\frac{\partial w}{\partial y} + w\frac{\partial w}{\partial z}\right) = -\frac{\partial p}{\partial x} + \rho g_z + \mu\left(\frac{\partial^2 w}{\partial x^2} + \frac{\partial^2 w}{\partial y^2} + \frac{\partial^2 w}{\partial z^2}\right) \qquad 9$$

The parabolic velocity profile for steady laminar flow in a cylindrical pipe is:

$$\frac{U}{u_{max}} = 1 - (\frac{r}{R})^2 \quad 10$$

$$u_{max} = 2 * V_{inlet} \quad 11$$

Depending upon the accurateness of experimental results and empirical correlations, whether to improvement meshing or whether or initial conditions or the boundary ones is decided. The reason of high dependency on empirical data is due to the association of randomness with turbulence. In turbulence there is no exact equation, all solutions are empirical data points. An example of this is the equation for skin friction for turbulence which is

$$\lambda = .3164(\frac{\overline{u}d}{v})^{-\frac{1}{4}} \frac{.3164}{Re^{.25}} \quad 12$$

The main reason that it is an empirical equation, it has a few limiting conditions. Some of those limiting conditions are that it has to be only for smooth pipes and it is only useful for Reynolds number less than 100,000.

Also, another very important one is Nikuradse's empirical correlation for turbulent flow which is given by

$$\frac{u}{U} = (\frac{y}{R})^{\frac{1}{n}} \quad 18$$

where n, the power-law exponent varies with respect to the Reynolds number. Turbulent cases are very difficult to analyze because there is no exact answer, however the Moody diagram in which the coefficient of friction with respect to the Reynolds number is displayed, serves as a reference as to what the solutions should appear to be. The Moody diagram is based off of

$$f = \phi(Re, \frac{\varepsilon}{D}) \quad 19$$

where the results are obtained from numerous set of experiments plotted on the Moody diagram.

3.3 Governing equations for entropy generation:

The equations used in CFD modeling are continuity equation, momentum equation and energy equation, which are all previously mentioned.

Equation used to calculate the entropy generation by viscous dissipation using a custom field function in CFD modeling is

$$S'''_{gen} = \left(\frac{\mu}{T}\varphi + \frac{\rho\varepsilon}{T}\right) + \left(\frac{k}{T^2}(\nabla T)^2\right) \quad 20$$

Where

$$\varphi = 2 * \left\{\left(\frac{\partial V_x}{\partial x}\right)^2 + \left(\frac{\partial V_y}{\partial y}\right)^2 + \left(\frac{\partial V_z}{\partial z}\right)^2\right\} + \left(\frac{\partial V_x}{\partial x} + \frac{\partial V_y}{\partial y}\right)^2 + \left(\frac{\partial V_y}{\partial y} + \frac{\partial V_z}{\partial z}\right)^2 + \left(\frac{\partial V_z}{\partial z} + \frac{\partial V_x}{\partial x}\right)^2 \quad 21$$

And

$$(\nabla T)^2 = \left\{\left(\frac{\partial T}{\partial x}\right)^2 + \left(\frac{\partial T}{\partial y}\right)^2 + \left(\frac{\partial T}{\partial z}\right)^2\right\} \quad 22$$

The entropy Generation term consists of two parts: Viscous dissipation and Thermal Dissipation.And again the viscous dissipation term consists of two parts, one is normal viscous dissipation ($\frac{\mu}{T}\varphi$) and another one is turbulent dissipation rate ($\frac{\rho\varepsilon}{T}$). Turbulent dissipation rate is due to the turbulence in the flow.

$$S'''_{gen,viscous} = \left(\frac{\mu}{T}\varphi + \frac{\rho\varepsilon}{T}\right) \quad 23$$

In isothermal case only viscous dissipation term comes into action. And for non-isothermal case along with the viscous term, thermal term is there.

$$S'''_{gen,thermal} = \left(\frac{k}{T^2}(\nabla T)^2\right). \quad 24$$

3.4 Equations for Pressure drop

Empirical method is used to calculate the pressure drop using the following equations

For straight pipe the Pressure drop is calculated as: $\frac{\Delta P_S}{L} = \frac{2f\rho\overline{V^2}}{D}$ 25

Or Hagen- Poiseuille equation for laminar flow $\Delta P_s = \frac{32\,L\mu\overline{V}}{D^2}$ 26

where f is the friction factor

for laminar flow $f = \frac{16}{Re}$ 27

for turbulent flow $\frac{1}{\sqrt{f}} = -2.0\log_{10}\left(\frac{\epsilon/D}{3.7} + \frac{1.256}{Re\sqrt{f}}\right)$ 28

For bending pipes head loss is calculated using the 3-K method and the pressure drop is calculated

Darby's 3-K method

$$K = \frac{k_1}{Re} + k_\infty \left(1 + \frac{k_d}{D_{in}^{0.3}}\right) \quad 29$$

Table 1: Constant values for 3-K method

angle	k_1	k_∞	k_d in$^{0.3}$	k_d mm$^{0.3}$
90^0, mitered one weld	1000	0.27	4	10.6
45^0, mitered one weld	500	0.086	4	10.6

Head loss due to bending: $h_l = K\frac{V^2}{2g}$ 30

Head loss due to straight Pipe: $h_p = \frac{2fLV^2}{g}$ 31

Total Head loss $h_{total} = h_l + h_p$ 32

Pressure Drop: $\Delta P_s = h_{total}\rho g$ 33

CHAPTER 4

Specification of Problem

4.1 Problem specification and Geometry Details:

Consider a steady state fluid flow through a pipe for different angle of pipe bending 'α' shown in the figure 1 and 2. The diameter and length of the channel are 2.5cm and 3.0 m respectively. The inlet velocity range is 0.0401923m/s to 1.004809m/s, which is constant over the inlet cross section. Pipe outlet is at pressure of 1 atm. As the fluid flows through the pipe, for a particular Reynolds number its corresponding average velocity is applied to the inlet of the pipe. For the case of isothermal, entropy generation is only due to viscous dissipation only. And for non-isothermal cases entropy generation is due to both viscous dissipation and thermal dissipation. So for each case its value is calculated and plotted and compared.

The computational domain of the cylindrical channels is represented in three dimensional (3D) by a cylinder the geometry consists of a wall, inlet and outlet.

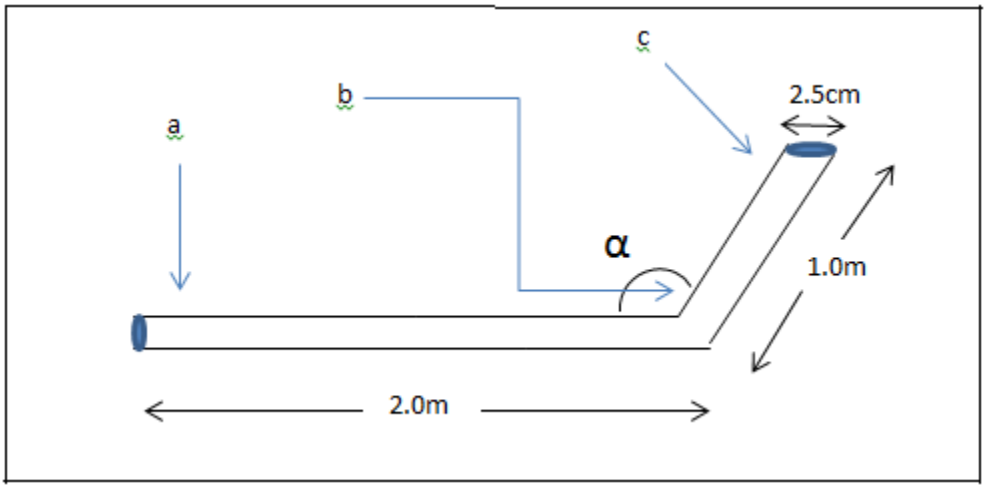

Figure 1 Geometry of the Pipe

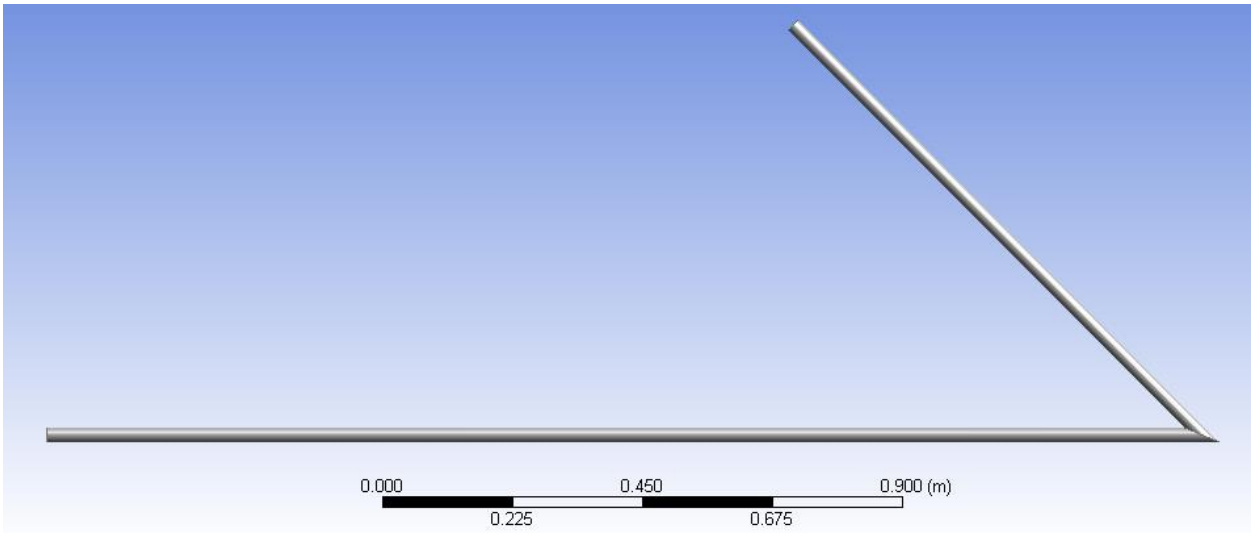

Figure 2 Geometry for $\alpha = 60^0$

4.2 Meshing of geometry:

Structured meshing method done in ANSYS Workbench was used for meshing the geometry.

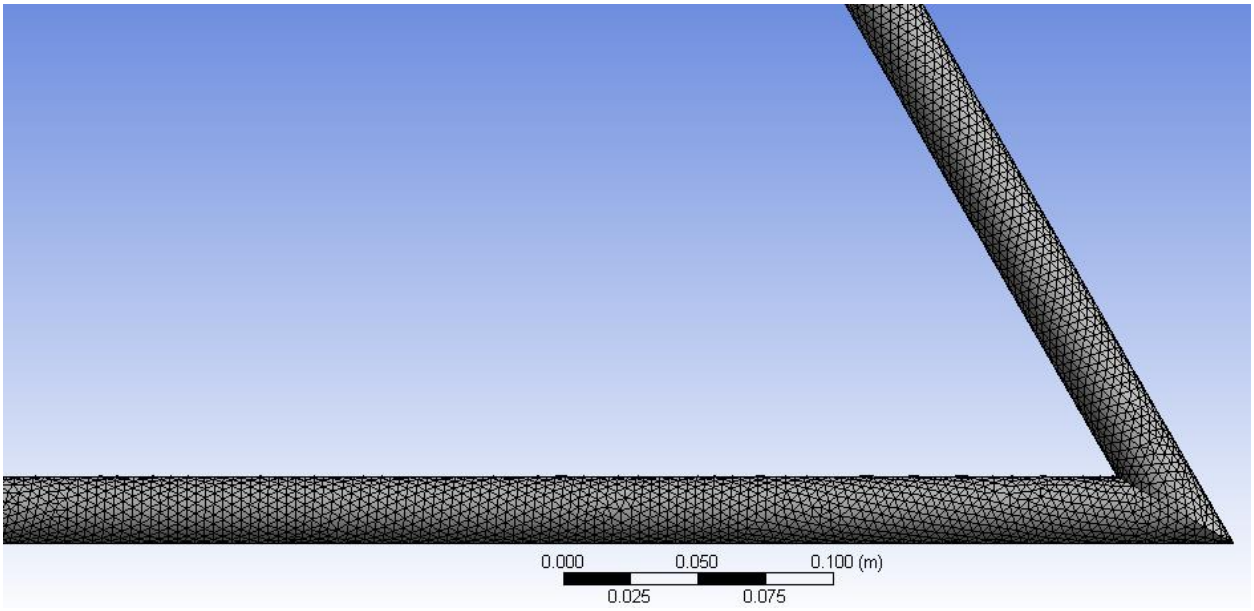

Figure 3 Meshing for $\alpha = 60^0$ bend pipe

4.3 Physical Model

Based on the Reynolds number,

$$Re = \frac{DV\rho}{\mu} \qquad 34$$

Where D is diameter of the pipe, ρ is the density and μ is the viscosity of the fluid. Either viscous laminar model or standard or k-ϵmodel is used for laminar and turbulent flow respectively.

Table 2: Choice of model based on Reynolds number

Reynolds No.(Re)	Flow Model
<2100	laminar
>2100	turbulent

4.4 Material Properties

The property of fluid is assumed to be constant for all the cases. Water based fluid properties:

Table 3: Property of fluid water

K_f (thermal conductivity, W/mK)	0.6
μ (viscosity, kg/ms)	0.001003
ρ (density, kg/m^3)	998.2
C_p(specific heat, Kj/kg K)	4.182

4.5 Boundary Conditions:

- at the wall: $V_r = 0$, $V_z = 0$
- at inlet where V_{x0} is a constant : $V_r = 0$, $V_x = V_{x0}$
- at the outlet section providing a fully developed flow condition: $\frac{\partial V_r}{\partial z} = 0$ $\frac{\partial V_x}{\partial x} = 0$
- iso-thermal flow no thermal boundry condition
- non-isothermal case, constant heat flux and constant wall temp are applied

- where V_r is the velocity in radial direction and V_x is the velocity in x direction

4.6 Method of solution:

There are two ways to solve the problem stated above: (i) analytical method and (ii) CFD method. In the present study the entropy generation for different Reynolds number (for a given inlet velocity of mass flow rate) to get a optimize value. And then to compare the analytical values of the pressure drop with the CFD values of the pressure drop. The entropy generation value for iso-thermal case is found out by the Equation 23 and for non-isothermal case the entropy generation value is found out by Equation 20.

The CFD method follows the use of commercial software ANSYS Fluent 15.0 to solve the problem. The specified solver in Fluent uses a pressure correction based iterative SIMPLE algorithm with 2^{nd} order upwind scheme. The convergence criteria vary with flow rate.

Chapter-5

Results and Discussion:

5.1 Validation

Pipes and pipe bendings contribute to major part of pressure drop as well as energy consumption. So it is better to know pressure drop in a piping system.

Simulations have been done for the 1-weld mitered bend pipe for α equals to 45^0, 90^0 and 180^0 straight pipe and pressure drop over pipe is calculated for different Reynolds number. Fig. 4, 5 and 6 comparing the pressure drop in fig 4 it is clear that the 180^0 shows the lowest pressure drop. The angle 45^0 bending pipe shows the highest pressure drop for a particular Reynolds number and the angle 90^0 bending have the pressure drop in between them.

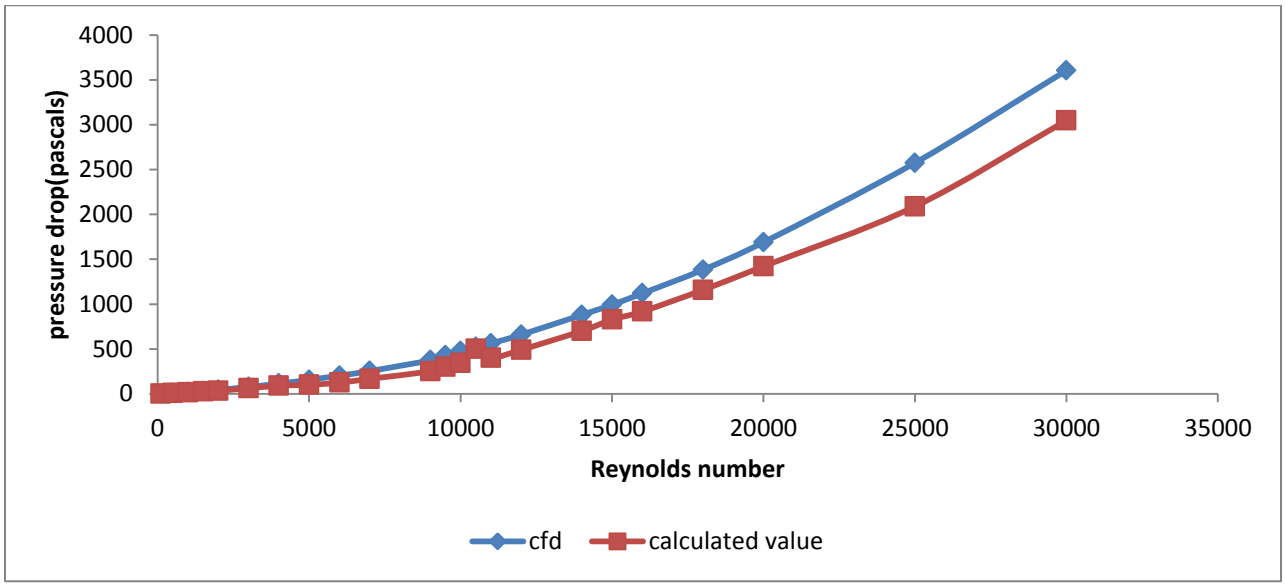

Figure 4 Pressure drop versus Reynolds number plot for α =45^0

For very low flow velocity the pressure drop is nearly same for all the angle of bending but difference in pressure drop among the bends increases as the velocity of the inlet fluid increases. And then the calculated pressure drops are compared with values of the simulation pressure drop.

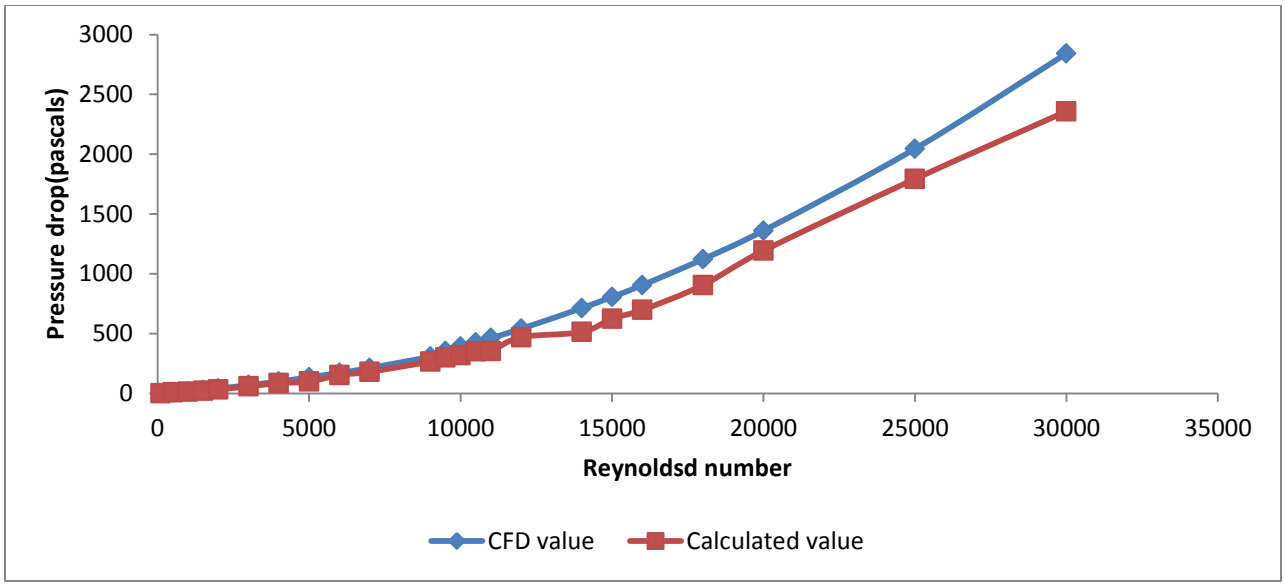

Figure 5 Pressure drop versus Reynolds number plot for α =90^0

In figure 4, 5 and 6 the values are compared and plotted for α =45^0, 90^0 and straight pipe 180^0 respectively. For low Reynolds number, the bending angles 45^0 and 90^0 the pressure drop values are nearly the same. For moderate pressure drop we find a little deviation among them. And for larger Reynolds number the difference grows larger. For the straight pipe up to moderate Reynolds number the pressure drop variation is negligible and for higher Reynolds number the difference in pressure drop gradually increases.

Table 4: Check For Mesh Independency by RMS error for straight pipe (α=180^0)

Case	Mesh Size	RMSD	NRMS %
1	72224	18.672	2.8754
2	121251	16.3185	2.513
3	218772	16.2563	2.503

Mesh independency are checked for α =180^0 for three different mesh sizes as given in Table 4. Pressure drop for each meshing is calculated for various Re and compared with corresponding pressure drop found from empirical equation. For each case RMS error or deviation and

NRMS% is calculated. Results show that for case 2 and case 3 NRMS values are nearly same. Therefor further simulations are done using case 2 mesh size.

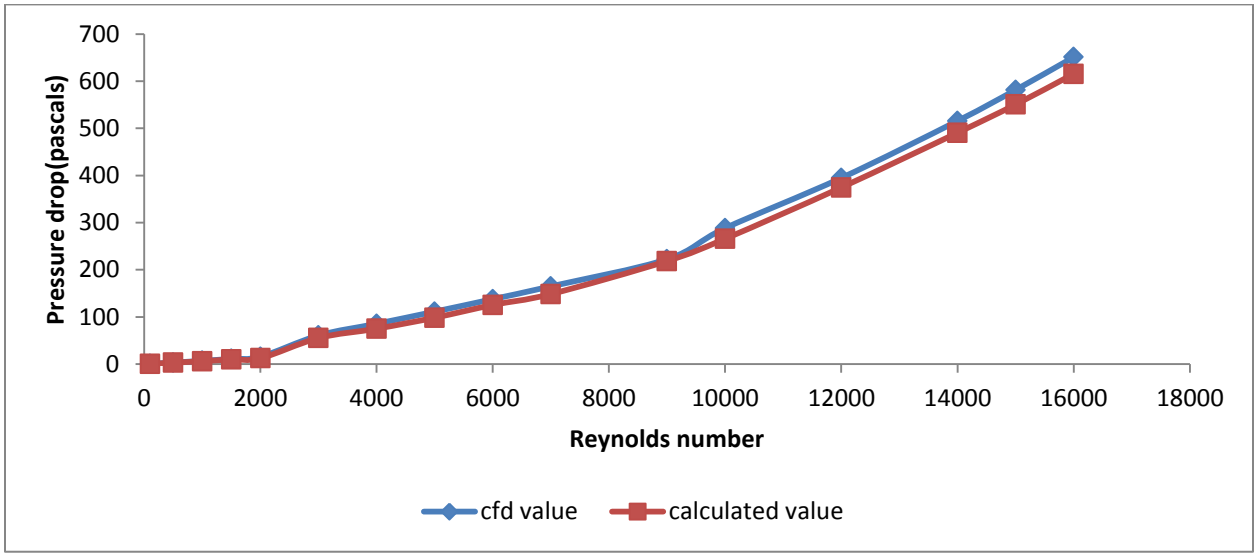

Figure 6 Pressure drop versus Reynolds number plot for α =180 ^{0}

5.2 prediction of entropy generation in pipefor isothermal boundary condition

The case is isothermal when the temperature is constant, i.e. the temperature of flowing fluid and wall/ surrounding are kept same. In this case both the temperature of the water and wall are at 300 K. The entropy generation is only due to the viscous dissipation. Dissipation or viscous dissipation is the source of energy supply to sustain turbulent flow. The turbulence dissipated rapidly as kinetic energy is converted to internal energy by viscous shear stresses hence the requirement of energy. But the temperature gradient developed due to this is very negligible. The viscous dissipation depends upon two things. One is the velocity gradient in all three directions ($\frac{\mu}{T}\varphi$) where φ is a function of velocity gradient and turbulent dissipation rate($\frac{\rho\varepsilon}{T}$).Both the viscous dissipation and turbulent dissipation rates increases as the flow rate increases, here it's the Reynolds number.

Considering the bending angle α= 90^{0}, from the curve in Figure 10, the entropy generation value increases as the Reynolds number increases.

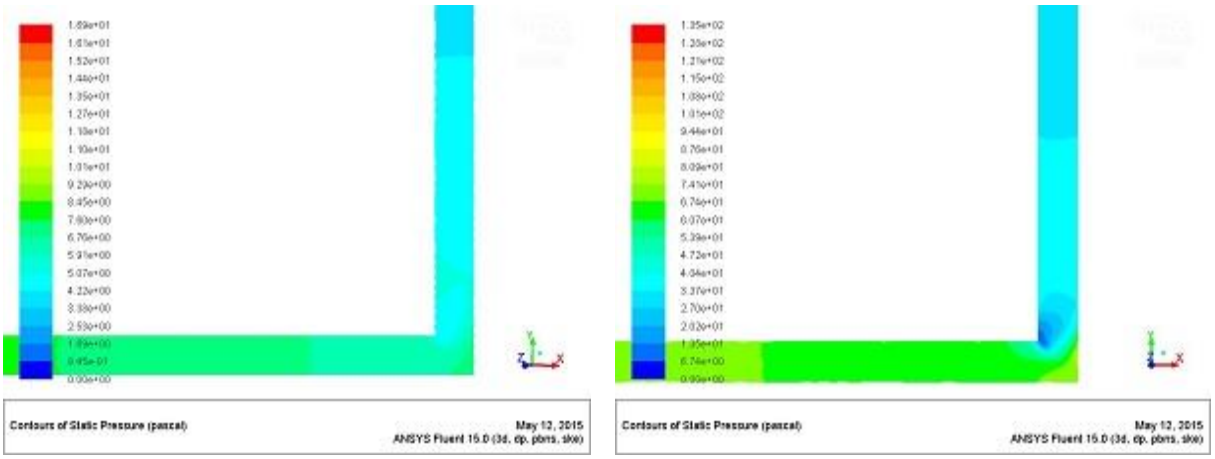

(I-b) (II-b)

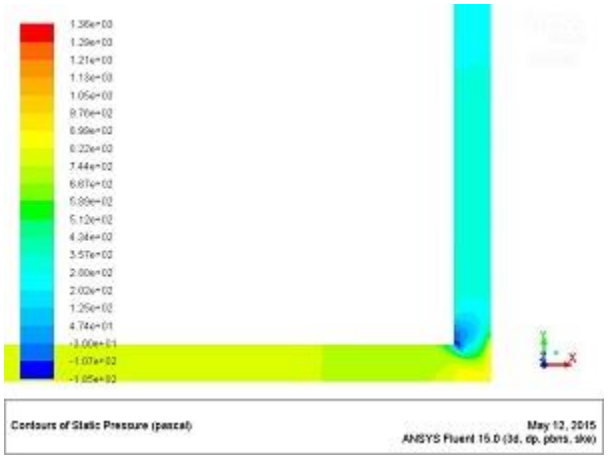

(III-b)

Figure 7 Contours of static pressure of $\alpha=90^0$ at point b of the channel for (I) Reynolds no 1000, (II) Reynolds no 5000 (III) for Reynolds no 20000

Figure 7 shows the contours of the pressure plot for Reynolds number 1000 and 5000. Pressure is highest at the inlet and lowest at the outlet and the pressure gradually decreases from inlet to outlet. As the Reynolds number increases the pressure drop also increases which can be clearly seen from Fig. 7 (I) and (II), the static pressure value is highest for Reynolds number 20000 followed by Re5000 and then 1000. At the bending position towards the outer wall near point (b), there is a small amount of increase and decrease in pressure, which is due to impact of the fluid on the wall.

The kinetic energy of the moving fluid gets converted into pressure energy and the pressure increases near the pipe bending. But at the same time at the opposite side of the wall there is a

little higher pressure drop than the normal where the pressure energy is converted into kinetic energy.

Figure.8 shows the velocity contour plot for α = 90° and *Re* = 1000, 5000 and 20000. For all the contour plots it is observed that the velocity magnitude is less near the wall (nearly zero) and highest at the center of the pipeline. As the wall is stationary frictional forces comes in to action on the moving fluid. But as the flow rate increases (here Reynolds number) the magnitude of velocity increases gradually from the wall to the center of the pipe.

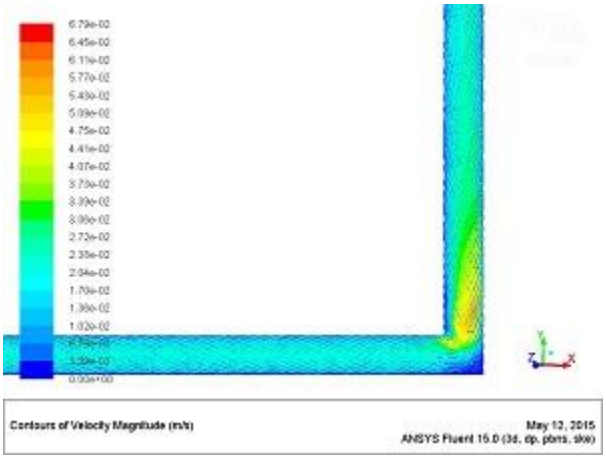

(I-b)

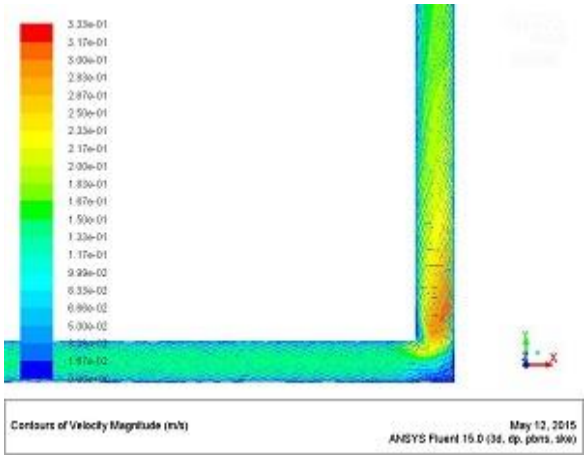

(II-b)

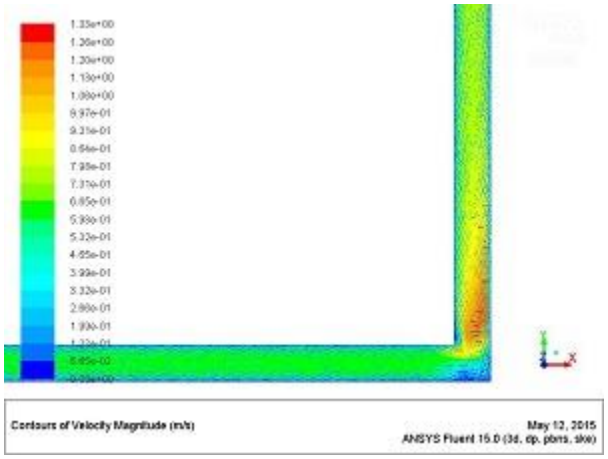

(III-b)

Figure 8 Velocity contours for α = 90^0 at point b of the channel for (I) for Reynolds number 1000, (II) for Reynolds number 5000, (III) for Reynolds no 20000

At the bending of the pipe, towards the outer wall the velocity magnitude increases as the potential energy of fluid transfers into the kinetic energy. Whereas at the other side of the wall of the bend there is a decrease in velocity magnitude. At the inlet the velocity magnitude is little higher than compared to other sections of the pipe. At the tip of bend, some vertex also forms due to change in shape of the pipe. And the velocity of the fluid is nearly zero at that point. As the Reynolds number increases the velocity magnitude also grows.

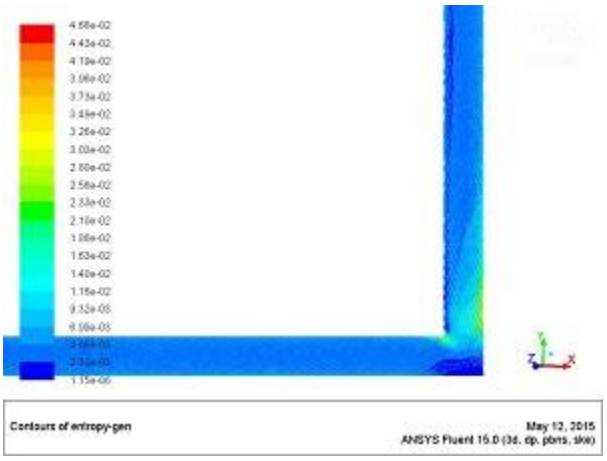

(I-b)

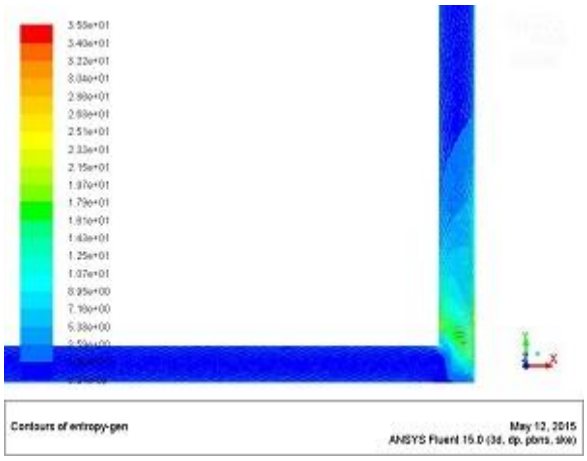

(II-b)

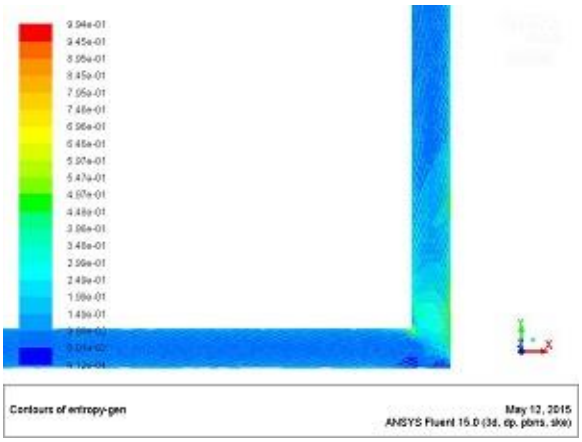

(III-b)

Figure 9 Contours of local entropy generation values for $\alpha = 90^0$at different points of the channel for (a) Reynolds no 1000 (b) Reynolds no 5000 (c) Reynolds number 20000

Figure. 9 shows contour plots of local entropy generation. There are two portion of the pipe that requires our attention. One is entrance region i.e. point (a) and another one is at the bending towards the wall of the pipe i.e. point (b). In the entrance region the entropy generation is due to

viscous force against the wall. In the entry region the velocity is higher and suddenly due to opposing frictional forces velocity gradients gets developed. The entropy generation is the function of square of velocity gradient (Eq. 23). While at the bending, it is due to a sudden change in pressure drop as well as the velocity magnitude. Kinetic energy gets converted into pressure energy and vice versa in that region. Due to these change in velocity magnitudes velocity gradient develop, hence the entropy generation which is a function of square of velocity gradient develops. Entropy generation rate near the wall increases sharply and decreases along the pipe. And in the fluid due shear stresses the velocity gradient is developed, but entropy generation values due to those are very small and can be neglected.

As the flow rate increases the magnitude of velocity increases accordingly velocity gradient also increases. Along with it the turbulent dissipation rate also rises once the flow is turbulent. As the entropy generation depends on both the viscous dissipation and turbulent dissipation rate for isothermal case the entropy generation rate also rise as the Reynolds number increases. From the figure.9 it is clear that the entropy generation values are more for higher Reynolds number.

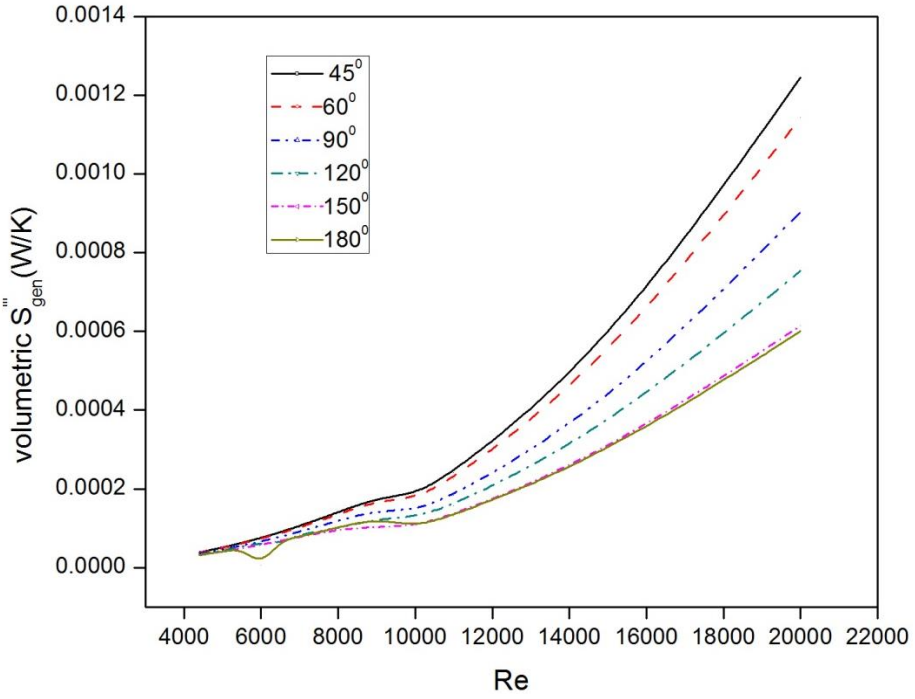

Figure 10 Curve between Reynolds number and volumetric entropy generation for different α

The entropy generation values for various bending angles are plotted against the Reynolds number as shown in Figure.10 shows a constant increase in the entropy generation values. Entropy generation value is highest for $\alpha = 45^0$ bend pipe and lowest for $\alpha = 180^0$ bend pipe, while others according to the increasing bending angle. But for Reynolds number near to 5000 the entropy generation value nearly same for all bending angles after that the difference in values rises as the bending angle increases.

5.3 Non-isothermal boundary condition

5.3.1 Prediction of Entropy generation for Constant heat flux wall

Heat transfer is a thermodynamic irreversibility in all engineering devices. When heat is transferred across a finite temperature difference, some capacity to do work is lost. And entropy is generated.

Thermal flux or heat flux is the rate of heat energy transfer through a given surface per unit area. It is a vector quantity. It is a derived quantity as it involves two quantities, heat transfer and area. Heat flux is important in energy balance calculations. Normally it is used to maintain or establish a steady state thermal gradient.

As the case is non-isothermal the temperature is not constant. Constant heat fluxes of different values are applied on the wall of the pipe. And the entropy generation is studied. Now the entropy generation is not only due to viscous dissipation but also for the thermal dissipation values$\left(\frac{k}{T^2}(\nabla T)^2\right)$.

The amount of entropy generated increases the loss of available work. So the entropy generation must be minimized to get optimum of the design of the thermal systems.

In the Fig. 11 contours of static temperature is plotted for bending angle 120^0 at wall flux of 10000 W/m^2 for Re=1000, 12000 and 30000. For Re 1000, Fig.11 (I) the temperature effect distribution can be clearly seen. Temperature profile in the pipe changes continuously. Temperature contours have high values in the surface region and as the distance from the pipe wall towards the pipe center increases its magnitude of temperature contours reduces. The temperature of the water gradually increases from the inlet towards the outlet.

Wall boundary condition is uniform heat flux. So the temperature of the wall rises continuously and heat is transferred form the wall to the fluid. Accordingly the temperature of the fluid is less in the entrance region and higher at the exit region.

Comparing the contours of Figure 11 (I) (II) and (III) the static temperature values are higher for low Reynolds number and low for higher Reynolds number. Residence time for low Reynolds number is high in comparison to the residence time for high Reynolds number. So fluids flow for low Reynolds number get more time for the transfer of heat into it.

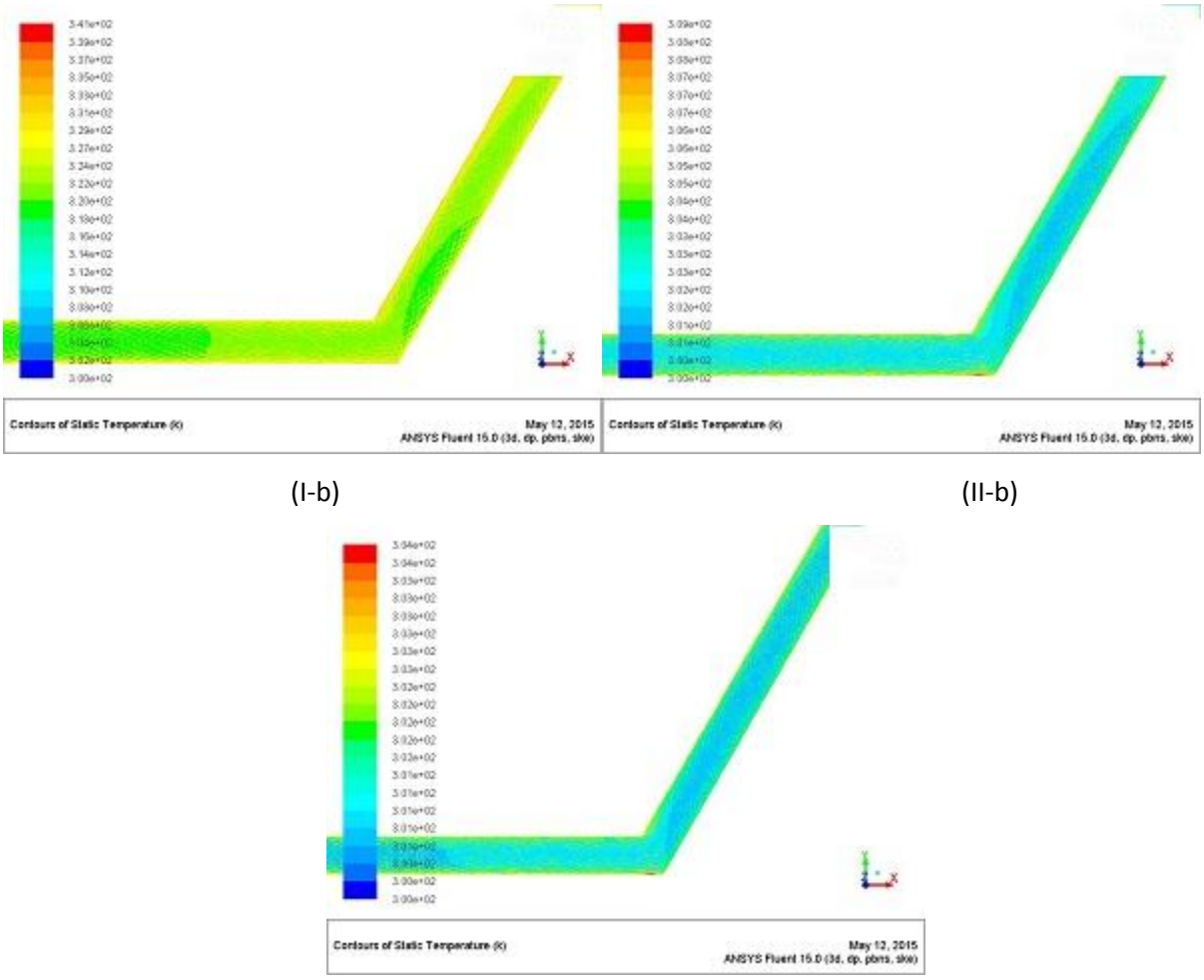

(I-b) (II-b)

(III-b)

Figure 11 Temperature contour $\alpha = 120^0$ and wall flux = 10000W/m^2 at different points of the channel for (I) Re= 1000, (II) Re=12000, (III) Re=30000

Figure12 Show the contour plots for thermal dissipation rates for α equals to 120^0 and constant wall flux of 10000 W/m^2. As we know from equation (20) thermal dissipation is a function of

temperature gradient. The more is the temperature variation the more will be the thermal dissipation. As in case of Re=1000, Fig. 12(I) the temperature variation along the pipe is more so the thermal dissipation value is higher. But for the Reynolds number 12000 and 30000 the temperature values decreases as well as the magnitude of temperature gradients also decreases. So the thermal dissipation rate is lower. So we can say that with rise in the Reynolds number the temperature variation becomes less and the thermal dissipation value decreases.

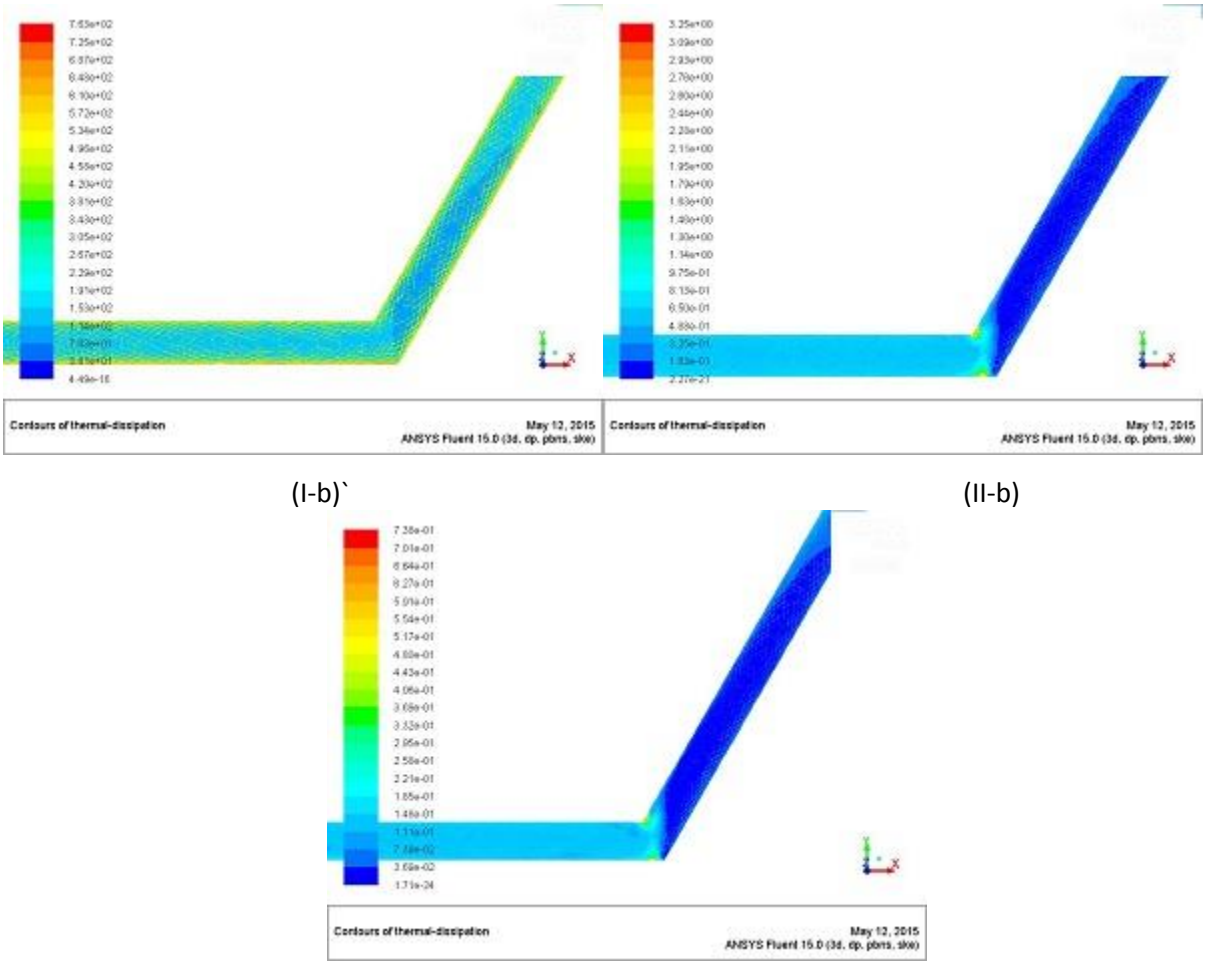

(I-b)`

(II-b)

(III-b)

Figure 12 Local thermal dissipation rate for bending angle $120^0$and wall flux 10000W/m^2at different points of the channel for(I) Re= 1000, (II) Re=12000

From the velocity contour plot for pipe with α = 120° and *Re* = 12000. For the contour plot it is observed that the velocity magnitude is less near the wall (nearly zero) and highest at the center of the pipeline. As the wall is stationary frictional forces comes in to action on the moving fluid. But as the Reynolds number (flow rate) the magnitude of velocity increases gradually from the

wall to the center of the pipe. At the bending of the pipe, towards the outer wall the velocity magnitude increases as the potential energy of fluid transfers into the kinetic energy. Whereas at the other side/ inner side of the wall of the pipe bend there is a decreases in velocity magnitude and rise in Static pressure magnitude. At the inlet the velocity magnitude is little higher than compared to other sections of the pipe. At the tip of bend, some vertex also forms due to change in shape of the pipe. And the velocity of the fluid is nearly zero at that point.

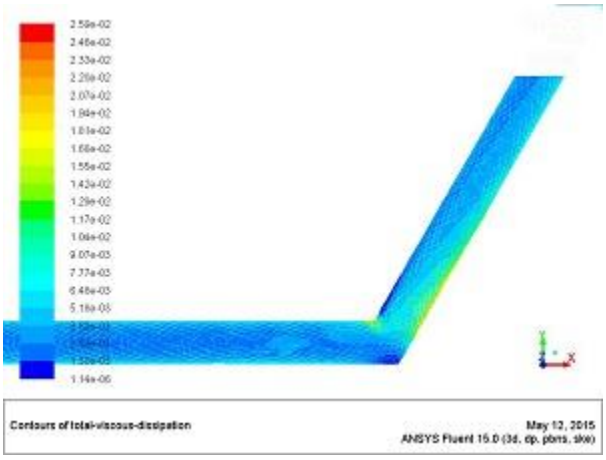

(I-b)

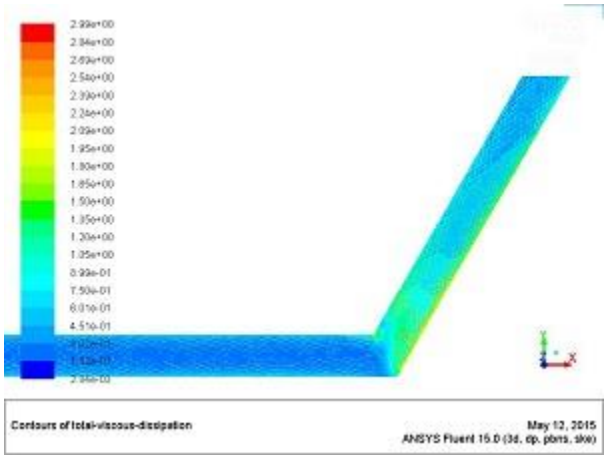

(II-b)

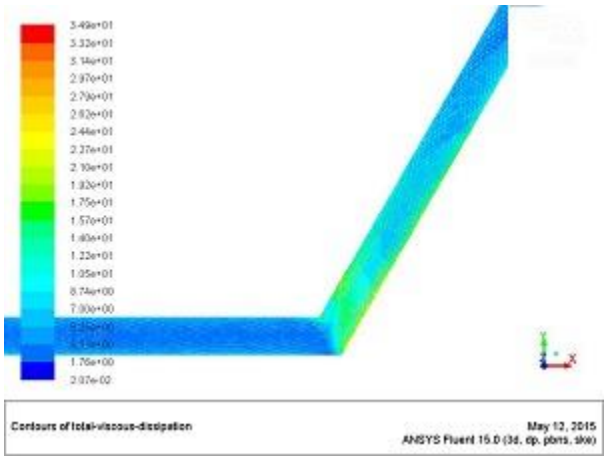

(III-b)

Figure 13 Contours of Local viscous dissipation rate for $\alpha = 120^0$and wall flux 10000W/m^2 at different points of the channel for (I) Re= 1000, (II) Re=12000, (III) Re=30000

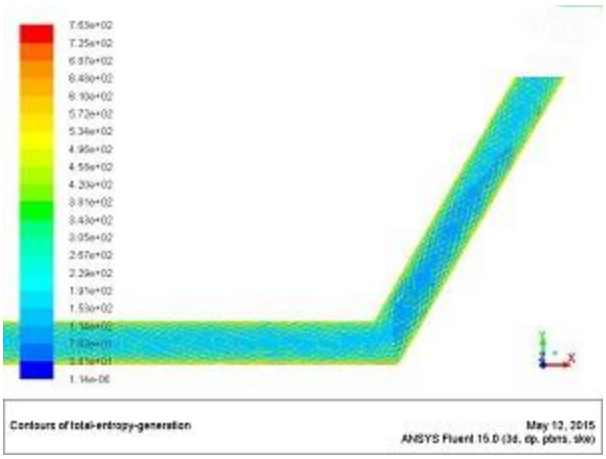

(I-b)

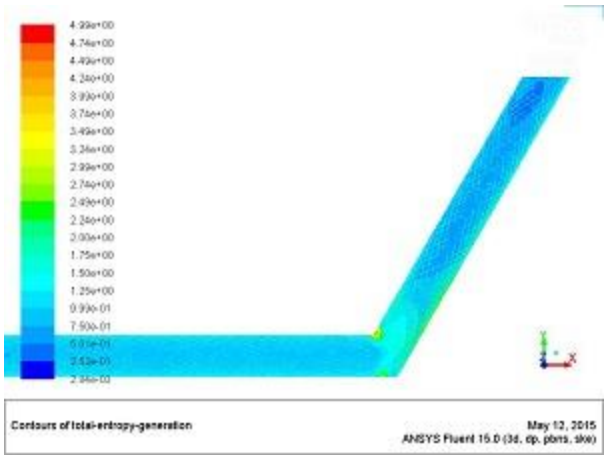

(II-b)

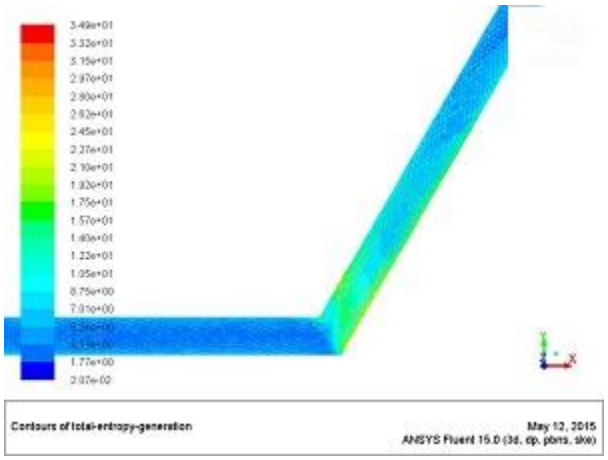

(III-b)

Figure 14 Contours of Entropy Generation for $\alpha = 120^0$ and wall flux 10000W/m^2 at different points of the channel for(I) Re= 1000, (II) Re=12000, (III) Re=30000

In the contours of entropy generation for low Reynolds number the entropy generation value is higher because of the thermal dissipation rate. Viscous dissipation have very little effect on the entropy generation for low Reynolds number. At the minimized entropy generation value as in Figure (13) both the viscous dissipation term and thermal dissipation term have nearly the same value. But for higher Reynolds number its value mostly depends upon the viscous dissipation.

The entropy generation value is the addition of viscous dissipation and thermal dissipation values. At low Reynolds number the viscous dissipation values are low but as the Re value increases entropy generation due to fictional losses increases. But at the thermal dissipation values are high for low Re and its value decreases as the Re decreases. So entropy generation minimization of occurs. In Figure 15 viscous dissipation, thermal dissipation and entopy

generation for constant wall flux of 1000 W/m^2 is plotted. And it can be clearly seen that entropy generation passes value at first decreasesand after reaching a optimum value it again increases..

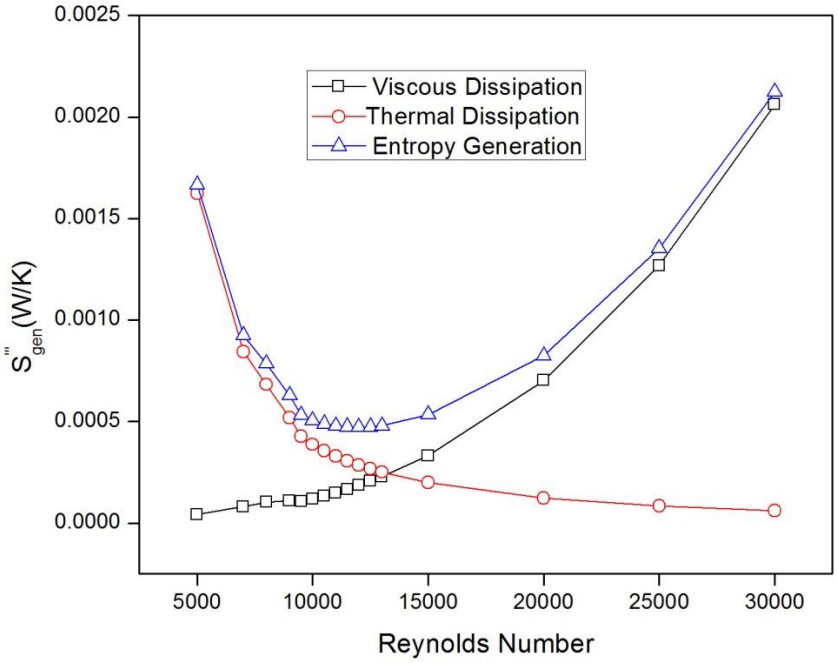

Figure 15 Curve between Reynolds number and volumetric entropy generation for $\alpha = 120^0$ angle of pipe bending at wall flux 10000W/m^2.

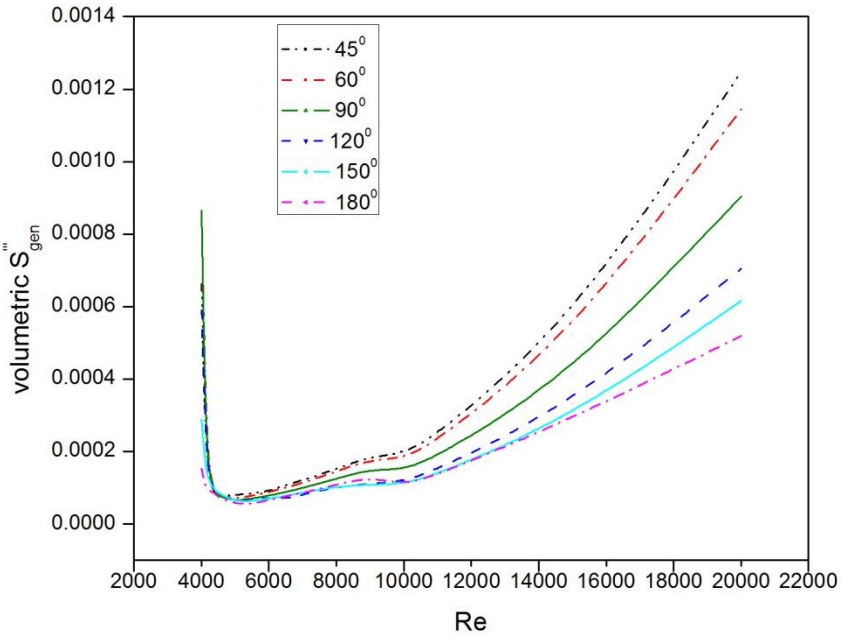

Figure 16 Curve between Reynolds number and volumetric entropy generation for different α at wall flux 1000W/m^2

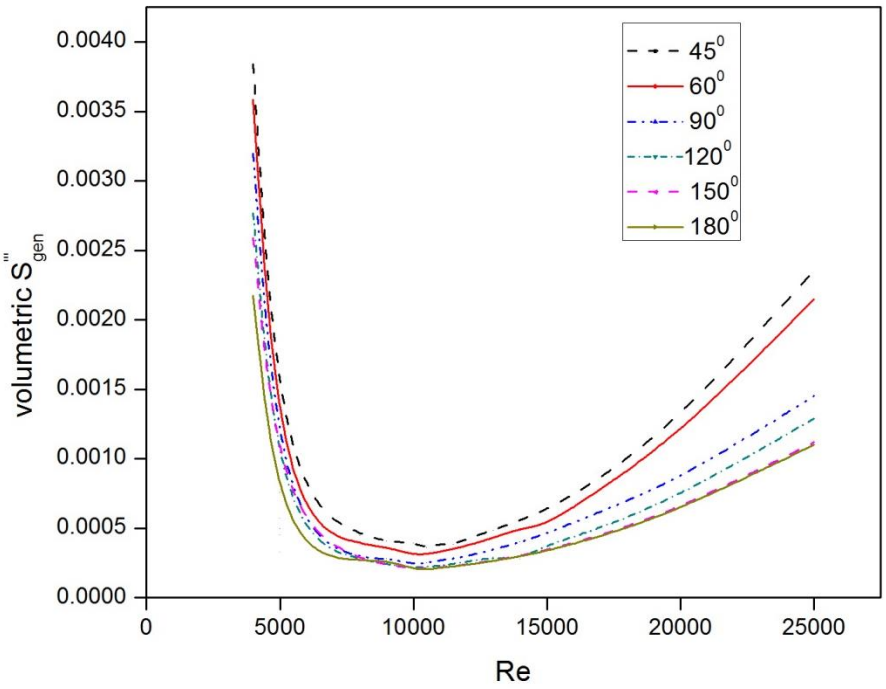

Figure 17 Curve between Reynolds number and volumetric entropy generation for different α at wall flux 5000W/m^2

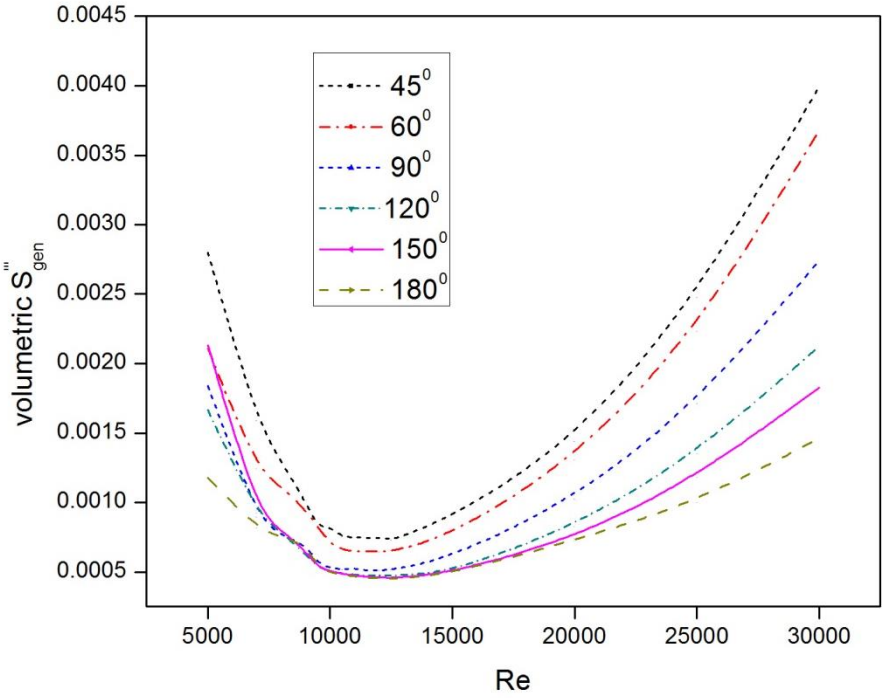

Figure 18 Curve between Reynolds number and volumetric entropy generation for different α at wall flux 10000W/m^2

Figure 16, 17, 18 and 19 represents the plot between volumetric entropy generation and Reynolds number for the entire bending angles considered at constant wall flux of 1000 W/m^2, 5000 W/m^2 10000 W/m^2 and 20000 W/m^2. And each case it is found that the entropy generation value decreases as the Reynolds number increases, then it reaches a minimum value and after that point the entropy generation value increases. Entropy generation value is maximum for $\alpha=45^{\circ}$ and lowest for $\alpha = 180^{\circ}$ and as the α value increases the entropy generation value decreases.

Here at the Reynolds number at which the entropy generation minimizes occur rises as the heat flux is increases, Figure 20. Due to increase in heat flux the temperature in the wall increases so heat is penetrated more to the water in comparison to lower heat flux. And thermal dissipation value is increased for higher heat flux. But to reach the optimum value of the entropy generation the frictional entropy generation value has to be increases. And this can be obtained only when the Re value is increased.

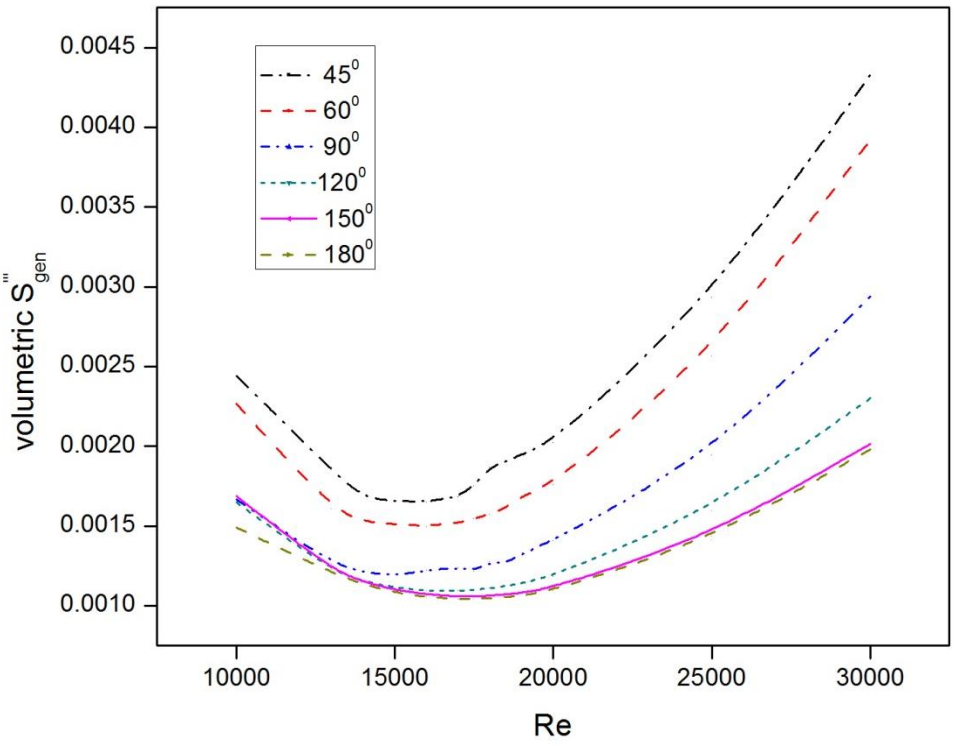

Figure 19 Curve between Reynolds number and volumetric entropy generation for different α at wall flux 20000W/m^2

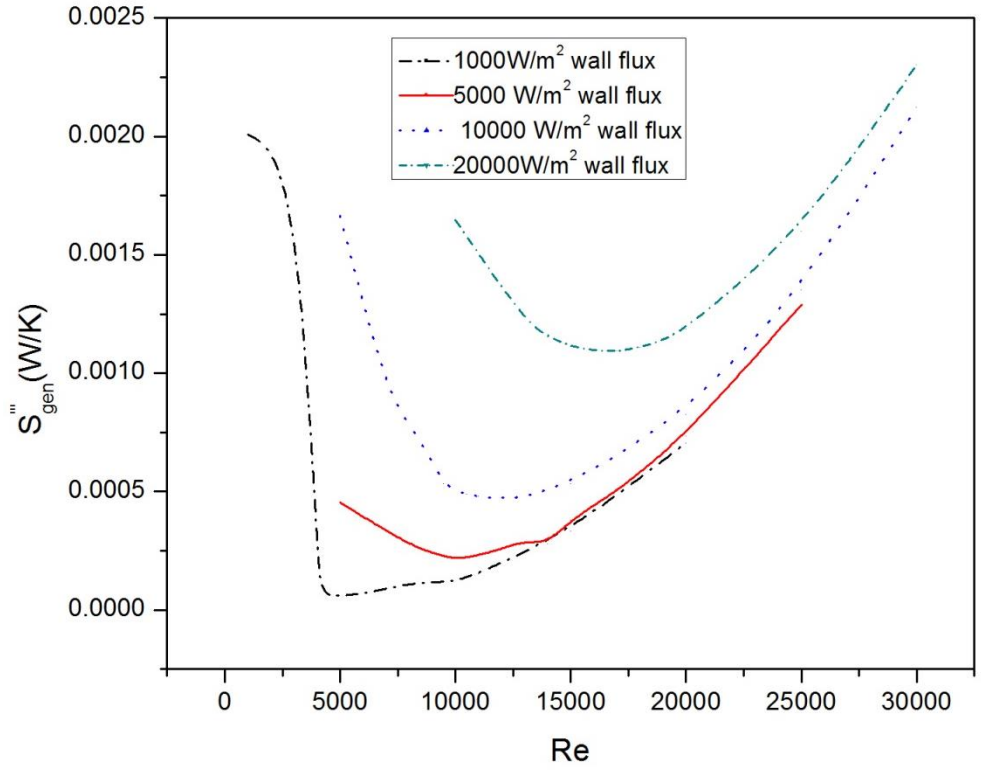

Figure 20 Entropy Generation versus Re plot for different wall flux for $\alpha = 120^0$

5.3.2 Prediction of Entropy generation for Constant wall Temperature

In the contours of static temperature the temperature effect distribution can be clearly seen. Temperature profile in the pipe changes continuously. Temperature contours have high values in the surface region and as the distance from the pipe wall towards the pipe center increases its magnitude of temperature contours reduces. The temperature of the water gradually increases from the inlet towards the outlet.

Wall boundary condition is uniform wall temperature. So due to temperature difference heat is transferred form the wall to the fluid throughout the duct. Accordingly the temperature of the fluid is less in the entrance region and higher at the exit region.

Comparing the contours of the static temperature values are higher for low Reynolds number and low for higher Reynolds number. Residence time for low Reynolds number is high in comparison to the residence time for high Reynolds number. So fluids flow for low Reynolds number get more time for the transfer of heat into it.

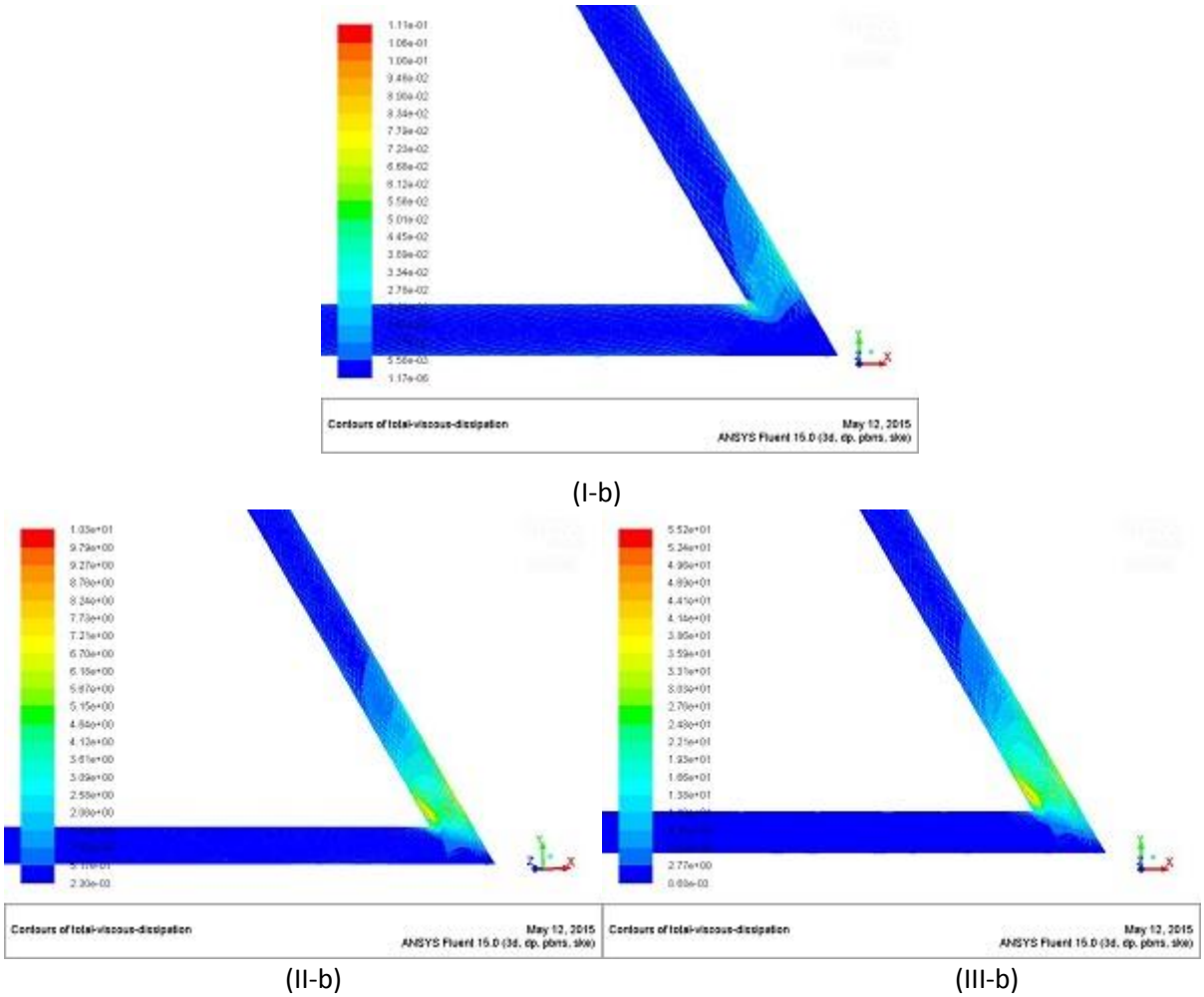

(I-b)

(II-b) (III-b)

Figure 21 Contours of Viscous dissipation for 60^0 bend wall temp=315K at different point-b of the channel (I) Re= 1000, (II) Re=11000, (III) Re=20000

From the contour plots for thermal dissipation rates for bending angle 60^0 and constant wall temperature 315K. As we know from equation (20) thermal dissipation is a function of temperature gradient. The more is the temperature variation the more will be the thermal dissipation. As in case of Re=1000, the temperature variation along the pipe is more so the thermal dissipation value is higher. But for the Reynolds number 12000 and 30000 the temperature values decreases as well as the magnitude of temperature gradients also decreases. So the thermal dissipation rate is lower. So we can say that with rise in the Reynolds number the temperature variation becomes less and the thermal dissipation value decreases.

The velocity magnitude is less near the wall (nearly zero) and highest at the center of the pipeline. As the wall is stationary frictional forces comes in to action on the moving fluid. But as

the Reynolds number (flow rate) the magnitude of velocity increases gradually from the wall to the center of the pipe. At the bending of the pipe, towards the outer wall the velocity magnitude increases as the potential energy of fluid transfers into the kinetic energy. Whereas at the other

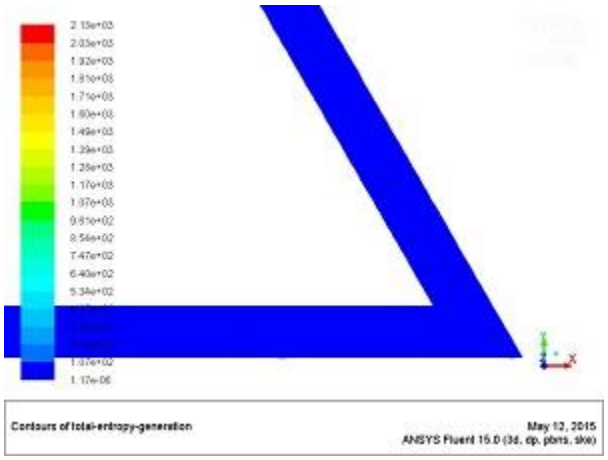

(I-a)

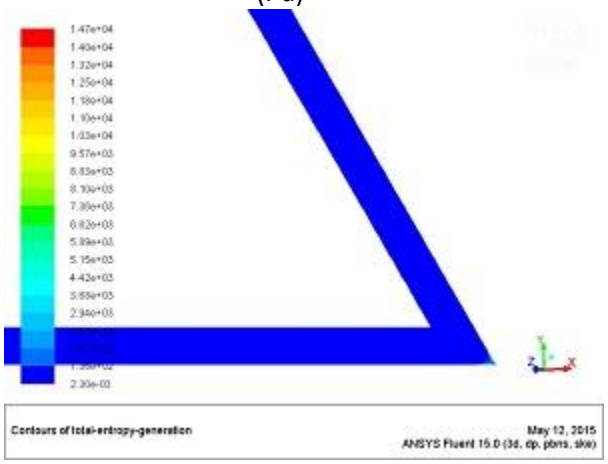

(I-c)

Figure 22 Contours of Entropy Generation for $\alpha = 60^0$ and wall temperature=315Kat different points of the channel for (I) Re= 1000, (III) Re=20000

From the contours of local viscous dissipation rates (Figure 22). As it depends upon the function φ and turbulent dissipation rate ε as in eq. 20 and 21. The viscous dissipation values are higher at the entrance region, near the wall and at the pipe bending. At the entrance region the fluid suddenly comes in contact with the stationary solid walls. And at the wall, which opposes the fluid motion by frictional action also increases the viscous dissipation. Near the pipe bending due to sudden change in geometry of the pipe, there is increase and decrease of pressure and velocity term which adds to the viscous terms and thus to entropy generation. The value of viscous

dissipation increases as the Reynolds number rises because velocity magnitude becomes higher and due to frictional forces velocity gradient also increases.

In the contours of entropy generation for low Reynolds number the entropy generation value is higher because of the thermal dissipation rate. Viscous dissipation have very little effect on the entropy generation for low Reynolds number. At the minimized entropy generation value as in both the viscous dissipation term and thermal dissipation term have nearly the same value. But for higher Reynolds number its value mostly depends upon the viscous dissipation.

In the Figure 23 the entropy generation due to friction or viscous dissipation and thermal dissipation are plotted verses Re. As the Re value increases the entropy generation due to frictional loss also increases but the increment is very slow. By increasing the Re the frictional losses increases and the value of velocity gradient accordingly increases. But for thermal dissipation, the value at first increases with increase in Re up to a point then suddenly decreases sharply. After that point it again decreases very slowly. This happens so because of the fact that for small Reynolds number the residence time of water in the pipe is more in comparison to higher Re number cases. Entropy generation is addition of those two values. So for low Re its value is high and totally depends upon the thermal dissipation value but for lower Re it depends upon the viscous dissipation.

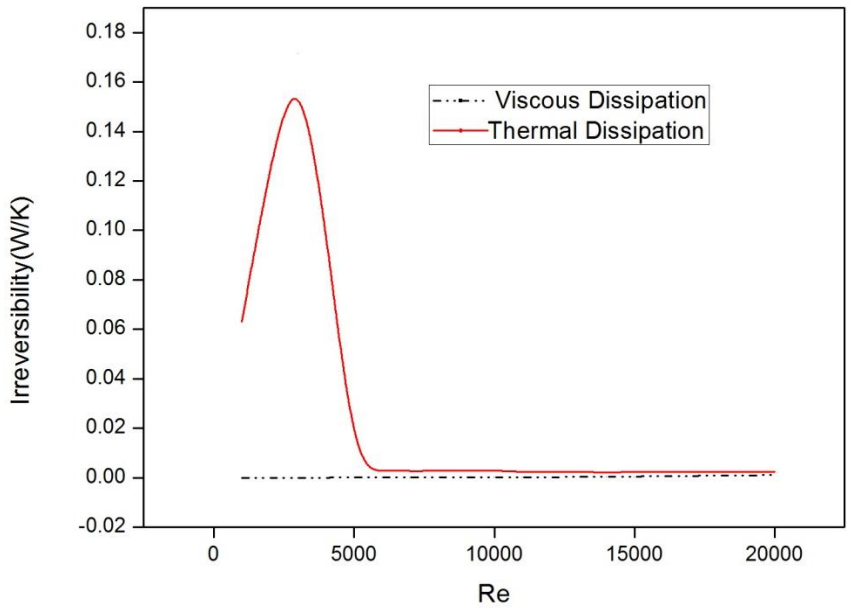

Figure 23 Curve between Reynolds number and viscous dissipation and thermal dissipation for α = 60^0 at wall Temp 315K

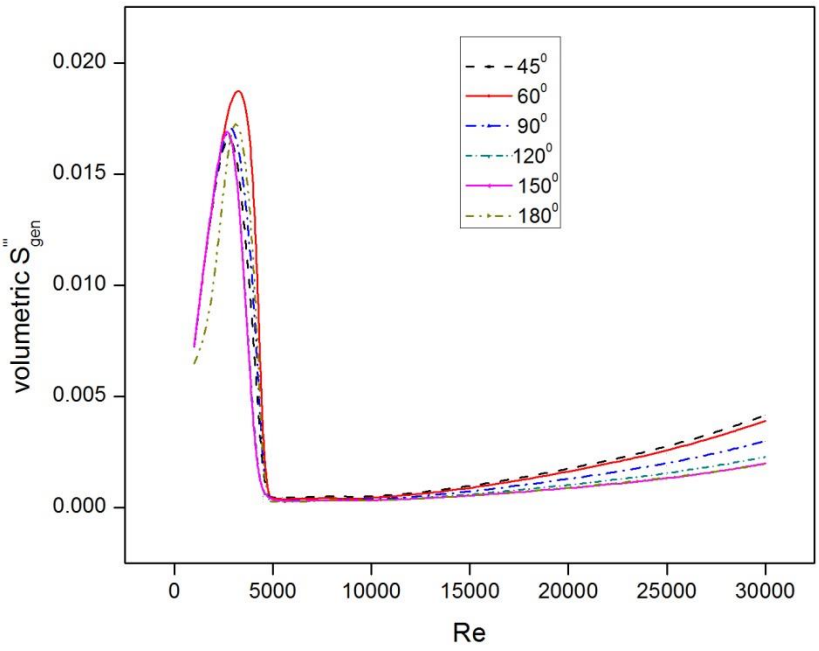

Figure 24 Curve between Reynolds number and volumetric entropy generation for different α at wall temp 305K

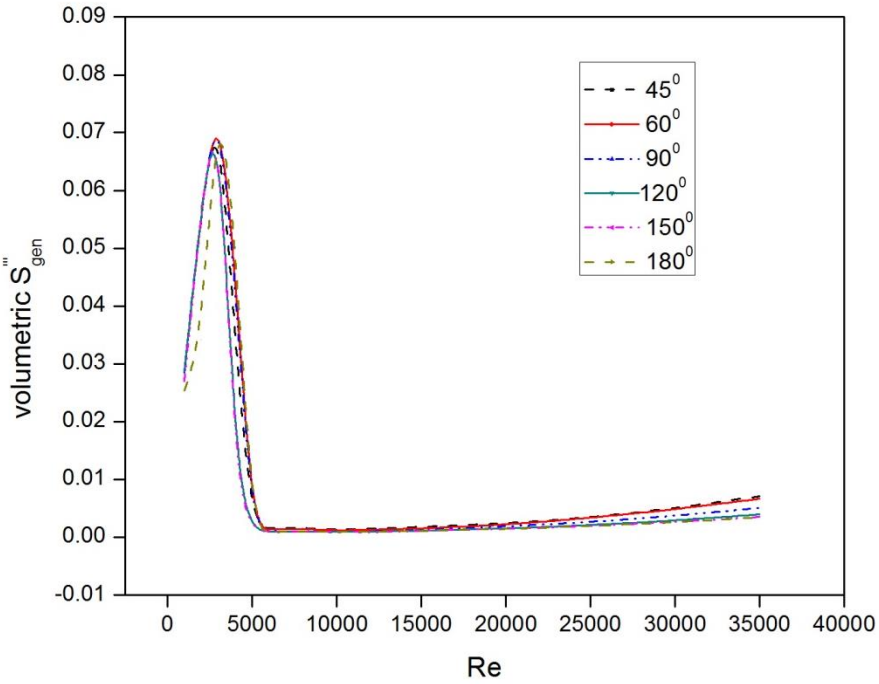

Figure 25 Curve between Reynolds number and volumetric entropy generation for different α at wall temp 310K

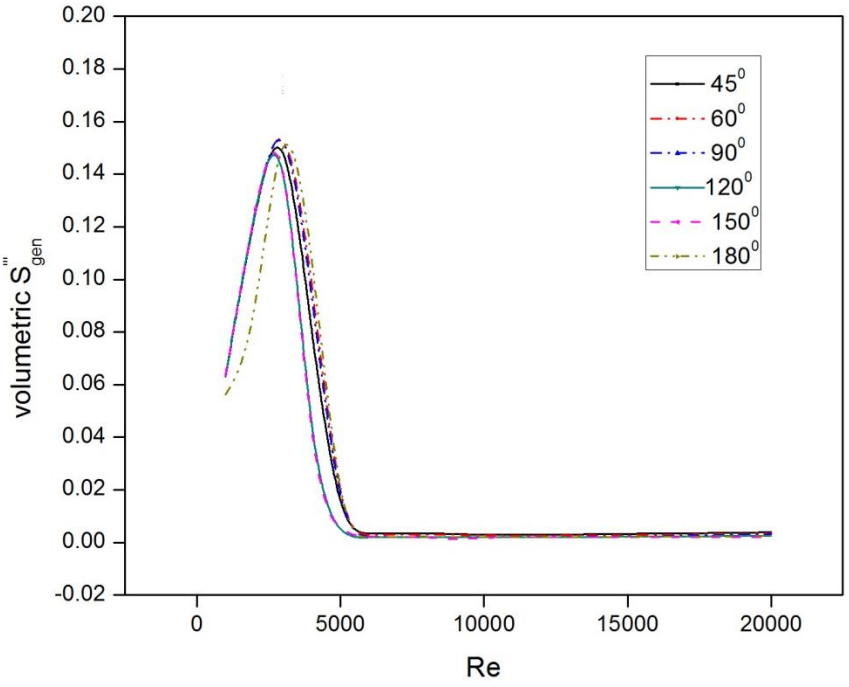

Figure 26 Curve between Reynolds number and volumetric entropy generation for different α at wall temp 315K

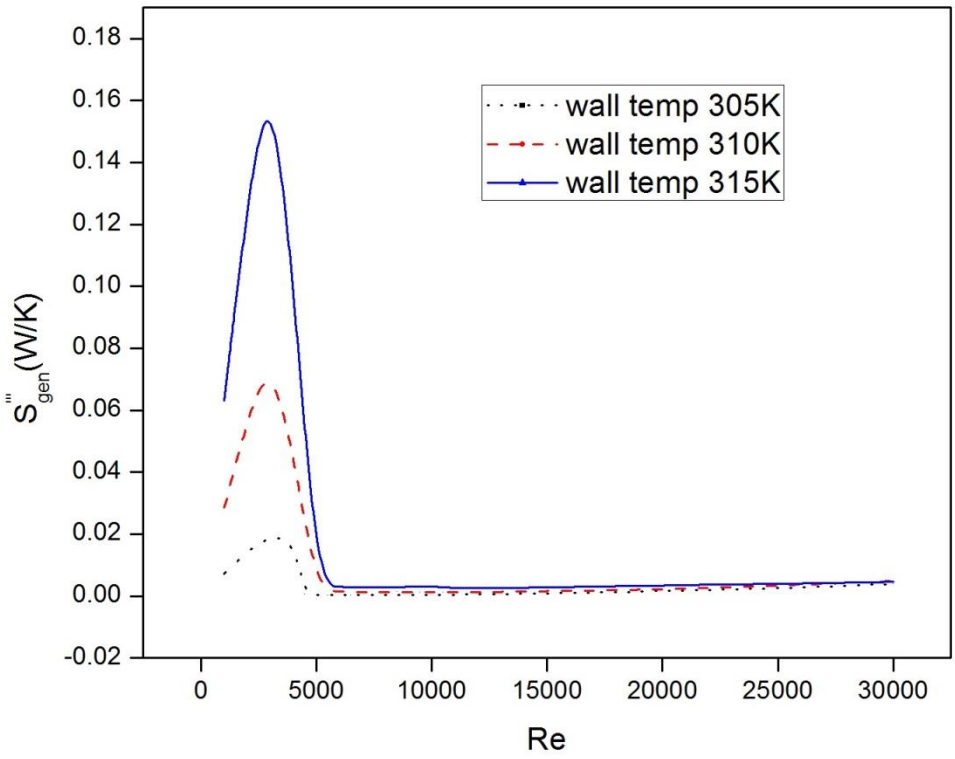

Figure 27 Curve between Entropy Generation and Re plot for different wall temperature for α $=60^0$

Figure. 25, 26 and 27 represents the plot between volumetric entropy generation and Reynolds number for the entire bending angles considered at constant wall flux of 305K, 310K and 315K. And each case it is found that the entropy generation value at first increases up to Re 3000 then it suddenly decreases and reaches a minimum value and after that point the entropy generation value increases very slowly. For $\alpha = 45^0$ bend has the highest entropy generation value and 180^0 has the lowest. As α value increases the entropy generation value decreases because with increase in α the frictional value decreases.

In figure 28 entropy generation is plotted against Re for $\alpha = 60^0$ for various wall temperature. As the wall temperature is increased the thermal dissipation component of the total entropy generation increases due to increase in temperature gradient within the fluid. As the temperature at the wall increases more heat is penetrated through the wall intro the fluid. SO the temperature gradient values also increases. But after reaching a maximum the entropy value decreases and attains minima. After it the values remains nearly constant or increases very slowly. The entropy generation rate is higher for higher wall temperature cases as the thermal component is greater for larger wall temperature.

Chapter-6

Conclusion:

Entropy generation is studied for the flow through a pipe with varying parameter α for three different cases (I) iso-thermal case, (II) isoflux (III) constant wall temperature case.

1. As the Reynolds number increases the pressure drop also found to be increased accordingly and it justifies all the pressure drop and velocity co-relations.
2. For isothermal (constant temperature throughout) case the entropy generation is due to frictional irreversibility only. The entropy generation value increases with increase in Re. with increase in Re the frictional forces increases and hence the velocity gradient.
3. The frictional component has two components. One is viscous dissipation and another one is turbulence dissipation rate. Turbulence dissipation rate only occurs when the flow is turbulent.
4. For lower α the frictional values are more. And as the value of α increases the entropy generation values decreases
5. For non isothermal case (both isothermal wall temperature and iso-flux case) the entropy generation value has two components. One is frictional irreversibility and other one is thermal irreversibility.
6. For low Re numbers the viscous dissipation contribution towards the total entropy generation rate is smaller in comparison to thermal dissipation component. Where as for large Re cases the contribution of thermal and viscous irreversibility is just reverse.
7. The thermal dissipation value does not depend upon the high or low temperature. It depends upon the temperature gradient. Total heat transfer is a function of the surface area and length of the duct along with the residence time.
8. As the value of heat flux or wall temperature increases, point where minimum entropy generation occur shifts towards higher Reynolds number.
9. Low is the angle α higher will be the entropy generation. And the value decreases as the α increases for a particular flow rate. The frictional contribution is higher for lower α values.

References:

[1] X Qian, Z Li, "Analysis of entransy dissipation in heat exchangers", International Journal Thermal Science, Volume 50, Pages 608–614, (2011)

[2] A Bejan., Entropy Generation Minimization, CRC press, (1996).

[3] A Bejan., A study of entropy generation in fundamental convective heat transfer, ASME Journal of Heat Transfer, Volume 101, Pages 718-725 (1979).

[4] A Bejan,., The concept of irreversibility in heat exchanger design: counterflow heat exchangers for gas-to-gas applications, ASME Journal of Heat Transfer, Volume 99, Pages 374-380 (1977).

[5] A. Z. Sahin , A second law comparison for optimum shape of duct subjected to constant wall temperature and laminar flow, Heat and Mass Transfer, Volume 33, Pages 425-430, (1998)

[6] I. Dagtekin, H. F. Oztop, A Z. Sahin, An analysis of entropy generation through a circular duct with different shaped longitudinal fins for laminar flow , International Journal of Heat and Mass Transfer, Volume 48, Pages 171–181, (2005)

[7] H. F. Oztop, Effective parameters on second law analysis for semicircular ducts in laminar flow and constant wall heat flux, International Communications in Heat and Mass Transfer, Volume 32, Issues 1–2, Pages 266–274, (2005)

[8] V. Zimparov, Extended performance evaluation criteria for enhanced heat transfer surfaces: heat transfer through ducts with constant wall temperature, International Journal of Heat and Mass Transfer, Volume 43, Issue 17, Pages 3137-3155, (2000).

[9].S. Mahmud, R. Andrew Fraser, The second law analysis in fundamental convective heat transfer problems, International Journal of Thermal Sciences, , The second law analysis in fundamental convective heat transfer problems, Volume 42, Pages 177–186, (2003)

[10] R. Ben-Mansour, A. Z. Sahin, Entropy generation in developing laminar fluid flow through a circular pipe with variable properties, Heat and Mass Transfer, Volume 42, Pages 1–11, (2005)

[11] P. K. Nag and P. Mukherjee, Thermodynamic optimization of convective heat transfer through a duct with constant wall temperature, International. Journal of Heat and Mass Transfer, Volume. 30(2), 405-408. (1987)

[12] A. Z. Sahin, Entropy generation and pumping power in a turbulent fluid flow through a smooth pipe subjected to constant heat flux, Exergy, An International Journal , Volume 2, Pages 314–321, (2002)

[13] J. A. Esfahani, A. Alizadeh Thermodynamic optimization of geometry in laminarconvective heat transfer through a pipe with constant wall temperature. In:Proceedings of the first international exergy, energy and environment symposium, Izmir, Turkey, Volume 77(3), Pages 13–17, (2003)

[14] A. Z. Sahin, S. M. Zubair, A. Z. Al-Garni, R. Kahraman, Effect of fouling on operational cost in pipe flow due to entropy generation, Energy Conversion and Management, Volume 41, Issue 14, Pages 1485–1496, (2000)

[15] A. Z. Sahin and R. Ben-Mansour, Entropy Generation in Laminer Fluid Flow Through a Circular Pipe, Entropy, Volume 5, Pages 404-416, (2003)

[16] B. F. Pussoli, J. R. Barbosa Jr, L. W. da Silva, M. Kaviany, Optimization of peripheral finned-tube evaporators using entropy generation minimization, International Journal of Heat and Mass Transfer, Volume 55, (25–26), Pages 7838–7846, (2012)

[17]G. Türkakar and T. O. Özyurt, Entropy generation analysis and dimensional optimization of an evaporator for use in a microscale refrigeration, International Journal of Refrigeration, (2015)

[18] H-Y Ye, K-S Lee, Refrigerant circuitry design of fin-and-tube condenser based on entropy generation minimization, International Journal of Refrigeration, Volume 35, Issue 5, Pages 1430–1438, (2012)

[19] G. P. Thiel, J. H. Lienhard, Entropy generation in condensation in the presence of high concentrations of noncondensable gases, International Journal of Heat and Mass Transfer
Volume 55, Issues 19–20, Pages 5133–5147, (2012)

[20] J. Christian, L. Hermes', W. de L. Silva Jr., F. A.G. de Castro, Thermal-hydraulic design of fan-supplied tube-fin condensers for refrigeration cassettes aimed at minimum entropy generation, Applied Thermal Engineering, Volume 36, Pages 307–313,(2012)

[21] A. Myat, K. Thu, Y. DeukKim, A. Chakraborty, W. G. Chun, K. C. Ng, A second law analysis and entropy generation minimization of an absorption chiller, Applied Thermal Engineering, Volume 31(14–15), Pages 2405–2413, (2011)

[22] K. H. Mistry, R. K. McGovern, G. P. Thiel, E. K. Summers, S. M. Zubair and J. H. Lienhard V, Entropy Generation Analysis of Desalination Technologies, Entropy, Volume 13, Pages 1829-1864, (2011)

[23] V. Bertola, E. Cafaro , A critical analysis of the minimum entropy production theorem and its application to heat and fluid flow, International Journal of Heat and Mass Transfer, Volume 51, Pages 1907–1912,(2008)

[24] G. Vučković, M. Banić, GradimirIlić, M. Vukić, M. Stojiljković, CFD Simulation of Local Entropy Generation Rate through Convective Heat Transfer in Parts of Steam Pipeline symposium, Subotica-Szabadka, EXPRES (2013)

[25] A. Tandiroglu, Effect of flow geometry parameters on transient entropy generation for turbulent flow in circular tube with baffle inserts, Energy Conversion and Management, Volume 48, Pages 898–906, (2007)

[26] X. T. Cheng, X. G. Liang, Discussion on the applicability of entropy generation minimization to the analyses and optimizations of thermodynamic processes, Energy Conversion and Management, Volume 73, Pages 121–127, (2013)

[27] T. A. Jankowski, Minimizing entropy generation in internal flows by adjusting the shape of the cross-section, International Journal of Heat and Mass Transfer, Volume 52, Pages 3439–3445, (2009)

[28] A. Z Sahin and B. S Yilbas, Entropy generation in the flow system generated in between two parallel plates due to bivertical motion of the top plate, SadhanaVol. 34 (3), Pages 455–466, (2009)

[29] S. Jarungthammachote, Entropy Generation Analysis of Transient Heat Conduction in a Solid Slab with Fixed Temperature Boundary Conditions, Wseas Transactions on Heat and Mass Transfer, Volume 9, (2014)

[30] G. Ibáñez, A. López, J. Pantoja, J. Moreira, J. A. Reyes, Optimum slip flow based on the minimization of entropy generation in parallel plate microchannels, Energy, Volume 50(1),Pages 143–149, 2013)

[31] G. Ibáñez, A. López, J. Pantoja, J. Moreira, Combined effects of uniform heat flux boundary condition and hydrodynamic slip on entropy generation in a microcahnnel, International Journal of Heat and Mass Transfer, Volume 73, Pages 201-206, (2014)

[32] T. W. Ting, Y. M. Hung, N Guo, Entropy generation of nanfluid flow with streamwise conduction in microchannels, Energy, Volume 64, Pages 979-990, 1 (2014)

[33]V. Anand, Slip law effects on heat transfer and entropy generation of pressure driven flow of a power law fluid in a microchannel under uniform heat flux boundary condition, Energy, Volume 76, Pages 716–732, 1 (2014)

[34] J. Guo, M. Xu, J. Cai, X. Huai, Viscous dissipation effect on entropy generation in curved square microchannels, Energy , Volume 36(8), Pages 5416–5423, (2011)

[35] E. Sciubba: Entropy Generation Minimization as a Design Tool. Part 1: Analysis of Different Configurations of Branched and Non-branched Laminar Isothermal Flow Through a Circular Pipe: International Journal of Thermodynamics, Volume. 14, Pages 11-20, (2011)

[36] J.D. Hilbert, Alternatives in pneumatic conveying pipeline bends, Bulk solids handling, Volume 4 (3), Pages 657-660, (1984).

[37] R.D. Marcus, J.D. Hilbert and G.E. Klinzing, flow through bends and acceleration zones in pneumatic conveying systems, bulk solids handling, Volume 5(4),Pages 769-779, (1985).

[38] A. Khapre, B. Munshi, Numerical investigation of hydrodynamic behavior of shear thinning fluids in stirred tank, Journal of the Taiwan Institute of Chemical Engineers, http://dx.doi.org/10.1016/j.jtice.2015.04.003, (2015)

[39] D. Rajavathsavai, A. khapre, B. Munshi, Numerical study of Vortex Formation inside a stirred tank, International Scholary and Scientific Research & Innovation, Volume 8(12), Pages 1393-1398, (2014)

[40] Albright's Chemical Engineering hand book, Table 5.7, pg 432, 3-K constant for loss coefficient for valve and fittings, Darby 3K method

[41] K.Y. Leong,R. Saidur, T.M.I. Mahlia, Y.H. Yau, Entropy generation analysis of nanofluid flow in a circular tube subjected to constant wall temperature, International Communications in Heat and Mass Transfer, Volume 39(8), Pages 1169–1175, (2012)

[42]K.Y. Leong, R. Saidur, M. Khairulmaini, Z. Michael, A. Kamyar, Heat transfer and entropy analysis of three different types of heat exchangers operated with nanofluids, International Communications in Heat and Mass Transfer, Volume 39, Issue 6, Pages 838–843, (2012)

[43] V. Bianco, O. Manca , S. Nardini, Entropy generation analysis of turbulent convection flow of Al_2O_3–water nanofluid in a circular tube subjected to constant wall heat flux, Energy Conversion and Management, Volume 77, Pages 306–314, (2014)

[44] P. K. Singh, K.B. Anoop, T. Sundararajan, S. K. Das, Entropy generation due to flow and heat transfer in nanofluids, International Journal of Heat and Mass Transfer, Volume 53,4757–4767, (2010)

[45] V. Bianco, S. Nardini and O. Manca, Enhancement of heat transfer and entropy generation analysis of nanofluids turbulent convection flow in square section tubes, Nanoscale Research Letters, Volume 6, 252-256, (2011)

[46]. V. Bianco, O. Manca and S. Nardini, Entropy generation analysis of turbulent convection flow of Al_2O_3–water nanofluid in a circular tube subjected to constant wall heat flux, Energy Conversion and Management, Volume 77, Pages 306–314, (2014).